

THESIS

IN VIVO REGULATION OF CHROMATIN DYNAMICS BY SACCHAROMYCES
CEREVISIAE HISTONE CHAPERONE NAP1

Submitted by

Kristi Barker

Department of Biochemistry and Molecular Biology

In partial fulfillment of the requirements

For the Degree of Master of Science

Colorado State University

Fort Collins, Colorado

Spring 2011

Master's Committee:

Advisor: Laurie Stargell

Karolin Luger
Carol Wilusz

ABSTRACT

IN VIVO REGULATION OF CHROMATIN DYNAMICS BY SACCHAROMYCES CEREVISIAE HISTONE CHAPERONE NAP1

Eukaryotic cells must organize massive amounts of DNA into the nucleus. In order to accomplish this, the DNA must be compacted into a highly ordered structure known as chromatin. The basic, repeating unit of chromatin is the nucleosome, which consists of two copies of each histone (H2A, H2B, H3 and H4) and organizes 147 base pairs of DNA. Due to its highly compact nature, nucleosomes must be removed during gene expression in order for the transcription machinery to access the DNA. Shuttling of nucleosomes on and off DNA is mediated by a group of proteins known as histone chaperones. Importantly, histone chaperones interact with another family of chromatin remodeling complexes known as histone acetyltransferases (HATs). Acetylation of histones is correlated with the active transcription of genes. The work presented here explores the dynamics and kinetics of histone H3 occupancy and acetylation of histone H3-K9 and H3-K14 in a wild-type strain and strains deleted for three known histone chaperones (Nap1, Vps75 and Asf1) of the yeast *Saccharomyces cerevisiae* at the well characterized galactose inducible genes. This data offers insight into the epigenetic regulation of chromatin as well as possible mechanisms for the histone chaperones surveyed.

ACKNOWLEDGEMENTS

I would like to express my gratitude to all who provided the opportunity and reinforced my ability to complete this thesis. First, I would like to thank Dr. Laurie Stargell, my thesis advisor, for the use of her lab facilities and for her knowledgeable guidance and timely words of encouragement. I applaud the time and dedication of my thesis committee members, Dr. Karolin Luger and Dr. Carol Wilusz. Additionally, I would like to recognize Colorado State University and the Department of Biochemistry and Molecular Biology for their approval of my request to conduct the research that supports the basis of this thesis. Finally, I would like to thank my friends and family who are always there for me.

TABLE OF CONTENTS

Abstract.....	ii
Acknowledgements.....	iii
Table of Contents.....	iv
CHAPTER 1 INTRODUCTION	
1.1 Eukaryotic Gene Regulation and Chromatin Structure.....	1
1.2 Chromatin Regulatory Proteins.....	2
1.3 Inducible Gene Expression: The Yeast <i>GAL</i> Genes.....	6
1.4 Gaps To Be Filled.....	6
CHAPTER 2 MATERIALS AND METHODS	
2.1 Yeast Strains and Media.....	10
2.2 Chromatin Immunoprecipitation Assay.....	10
2.3 Western Blot Assay.....	11
2.4 Fluorescence Assays.....	11
2.5 Cell Imaging.....	12
2.6 Data Analysis.....	12
CHAPTER 3 HISTONE EVICTION AND MODIFICATIONS AT GALACTOSE INDUCIBLE GENES	
3.1 Abstract.....	16
3.2 Introduction.....	16
3.3 Results.....	17
3.4 Discussion.....	34

CHAPTER 4 NAP1 CONTRIBUTIONS TO HISTONE EVICTION AND MODIFICATIONS AT GALACTOSE INDUCIBLE GENES

4.1. Abstract.....37
4.2. Introduction.....37
4.3 Results.....38
4.4 Discussion.....53

CHAPTER 5 HISTONE CHAPERONES ASF1 AND VPS75: CONTRIBUTIONS TO HISTONE EVICTION AND MODIFICATIONS AT GALACTOSE INDUCIBLE PROMOTERS

5.1 Abstract.....57
5.2 Introduction.....57
5.3 Results.....58
5.4 Discussion.....61

CHAPTER 6 CHARACTERIZATION OF HISTONE CHAPERONE-GFP FUSION PROTEINS

6.1 Abstract.....65
6.2 Introduction.....65
6.3 Results.....67
6.4 Discussion.....71

CHAPTER 7 FUTURE DIRECTIONS

7.1 Significance.....73
7.2 Discussion.....74

SUPPLEMENTAL

Real-Time PCR Oligomers Table.....76
Histone H3 Occupancy Tables.....77
Histone H3 Acetylation Tables.....81
Histone H3 Global Expression Levels.....87

References.....88

CHAPTER 1 INTRODUCTION

1.1 EUKARYOTIC GENE REGULATION AND CHROMATIN STRUCTURE

Inside the nucleus of eukaryotic cells, DNA and proteins are organized into chromatin. The basic level of organization is a histone octamer (two of each histone H2A, H2B, H3, and H4), which organizes 147 base pairs of DNA in two super-helical turns to create the nucleosome core particle ¹. Nucleosomes have a large impact on the accessibility of DNA, which influences gene regulation, DNA damage repair, and other nuclear functions that require access to DNA. Although nucleosomes were characterized as the basic unit of chromatin over 30 years ago and their structure is known in detail ^{1;2} there is still much to learn about how proteins regulate chromatin structure and, ultimately, gene expression. Chromatin architectural alterations occur as a result of post-translational modifications and/or the addition and removal of histones. Histone acetyltransferases (HATs) and histone chaperones are accessory proteins that are responsible for regulating these changes in chromatin structure. Histone chaperones modify the chromatin structure by assembling or disassembling nucleosomes during DNA replication, cell-cycle progression, and gene transcription (Table 1.1). HATs acetylate conserved lysine residues by catalyzing the addition of an acetyl group to the ϵ -amino group of histone tails (Table 1.2). It is unclear how histone chaperones and HATs modify and mobilize histones, and together regulate chromatin structure.

There are two mechanisms by which histone tail acetylation influences chromatin structure. Modifications of lysine residues function either by disrupting histone-DNA contacts or by influencing the recruitment of chromatin remodeling proteins. Chromatin is stabilized by electrostatic interactions between basic histone tails and acidic regions on adjacent nucleosomes. The effect of charge neutralization is disrupted by histone acetylation. Thus, neutralizing the positive charges of lysine residues by acetylation alters the interaction between the histone and the

negatively charged DNA backbone. As a result, the compacted chromatin (heterochromatin) is destabilized and “relaxed” (euchromatin). Furthermore, the exceptional diversity seen within patterns of histone marks at distinct residues comprises the histone code. This hypothesis states that histones are subjected to post-translational modifications, which lead to the recruitment of protein complexes that regulate chromatin structural states. Interestingly, histone acetylation signals for the recruitment of proteins that contain a bromodomain. Components of the Swi/Snf (SWItch/Sucrose Non-Fermentable) and RSC complexes (Chromatin Structure Remodeling Complex), and many transcription co-factors such as Gcn5 and p300 contain bromodomains ³.

1.2 CHROMATIN REGULATORY PROTEINS

HISTONE CHAPERONES MEDIATE HISTONE ASSEMBLY AND DISSASSEMBLY

The histone chaperone, Nap1 (Nucleosome Assembly Protein 1), promotes nucleosome assembly by preventing nonproductive nucleosomal interactions between H2A-H2B dimers and DNA, both *in vitro* and *in vivo* ⁴. Nap1 has been identified in all eukaryotes and its function is highly conserved ⁵. Nap1 disassembles nucleosomes that are acetylated at histone H3-K14 *in vitro* ⁶. Furthermore, Nap1 regulates cell-cycle progression ⁷ and nucleosome sliding within the nucleus ⁸, but also functions in the cytoplasm where it assembles the septin complex at the bud neck during daughter cell formation ⁹. Vps75, Vacuolar Protein Sorting 75, belongs to the NAP family of histone chaperones and is conserved from yeast to humans ^{10; 11}. Vps75 binds H3-H4 tetramer in contrast to other Nap1 family members which prefer the H2A-H2B dimer ^{12, 13} and can assemble nucleosomes *in vitro* ¹⁴.

TABLE 1.1: YEAST HISTONE CHAPERONES NAP1, Vps75, AND ASF1

HISTONE CHAPERONE	HISTONE BINDING PREFERENCE
Asf1	H3-H4
Nap1	H2A-H2B
Vps75	H2A-H2B

TABLE 1.2 HISTONE ACETYLTRANSFERASES IN YEAST

FAMILY	HAT	COMPLEX	SPECIFICITY
GNAT	Gcn5	SAGA	H3-K9, H3-K14, H3-K18
GNAT	Elp3	Elongator	H3-K14; H4-K8
MYST	Esa1	NuA4	H4-K5, H4-K8, H4-K12
P300/CBP	Rtt109	*	H3-K9, H3-K56

Asf1, Anti-Silencing Function 1, was initially characterized genetically in budding yeast as a suppressor of gene silencing when over-expressed¹⁵. More recently, Asf1 has been shown to act as a global chromatin disassembly factor¹⁶. Asf1 has been implemented in both replication-dependent and replication-independent chromatin assembly¹⁷. Chromatin immunoprecipitation (ChIP) experiments show that Asf1 is involved in transcription-coupled exchange of histone H3 at the *GAL1, 10* locus¹⁸. Specifically, Asf1 aids in the disassembly of histone H3 during active transcription and assembly of H3 during transcription repression. Furthermore, Asf1 increases the rate of histone eviction during the induction of yeast *PHO5* and *PHO8* promoters¹⁹.

HISTONE ACETYLTRANSFERASES LINK HISTONE MODIFICATIONS TO GENE EXPRESSION
HATs are classified into three distinct families GNAT, MYST, and P300/CBP (Table 1.2). The GNAT family (Gcn5-related N-acetyltransferases) is a diverse family of HATs. Gcn5 is part of the multiple subunit complex, SAGA, which functions during transcription²⁰. Gcn5 acetylates histones H3 lysine nine (H3-K9) and H3 lysine 14 (H3-K14)^{21; 22}. The MYST family is named for its founding members MOZ, Ybf2/Sas3, Sas2, and Tip60. The MYST family of HATs acetylates H4 and the histone variant Htz1^{23; 24}. Another HAT family consists of CREB binding protein (CBP) and p300, which acetylate histone H3-K9 and H3-K56^{25; 26}. One characteristic of many HATs is that they do not function independently *in vivo*. HATs are found in complex with other HATs, co-activators, and histone chaperones. Proteins found in complex with HATs are major elements specifying HAT substrate preference, and the functions of HATs depend primarily on the other protein subunits. For example, Gcn5 alone acetylates free histones H3-K14, as part of the SAGA complex with Ada2 and Ada3 it acetylates H3-K9, H3-K14, H3-K18 and H3-K23.^{27; 28}.

HISTONE ACETYLATION AND EVICTION REGULATE GENE EXPRESSION

Histone acetylation and eviction has been shown to play a regulatory role in transcription. *In vivo*, acetylated nucleosomes are evicted from the promoter and

coding region at a rate that correlates with gene transcription^{29; 30}, whereas deacetylated nucleosomes indicate the repressed state of a gene. Like histone acetylation, histone exchange influences transcription regulation. Nucleosomes are repressive to transcription initiation, as they control the access of regulatory proteins to promoter DNA and prevent the assembly of pre-initiation complexes. Additionally, nucleosomes must be removed from coding regions to allow the passage of RNA polymerase II. Thus, promoter and coding region chromatin disassembly is a globally used mechanism to regulate eukaryotic transcriptional induction.

1.3 INDUCIBLE GENE EXPRESSION: THE YEAST *GAL* GENES

The galactose inducible genes (*GAL1*, *GAL10*, and *GAL7*) encode the enzymes and regulators needed to utilize galactose as a carbon source³¹. The *GAL* genes are examples of well-studied genes whose expression is repressed by positioned nucleosomes at promoter and coding regions when cells are grown raffinose (Fig. 1.1). *GAL1* and *GAL10* are divergently transcribed and share an upstream activating sequence (UAS) containing four binding sites for the activator Gal4^{32; 33; 34}. When cells are grown in raffinose, Gal4 is expressed and binds the UAS, but the inhibitor Gal80 interacts with the activating region. Addition of galactose inactivates Gal80, thereby freeing Gal4 to activate transcription. However, nucleosomes that occupy the galactose inducible promoter must be modified and displaced for gene activation to occur. It is known that deletion of histone chaperone *NAP1* plays a direct role in the expression of galactose inducible genes *in vivo*⁴. More specifically, cells lacking Nap1 has increased transcription activation kinetics that fails to repress as quickly as wild-type cells. We will use this inducible gene system to evaluate the changes in histone occupancy and acetylation that occur upon gene activation (Fig. 1.2).

1.4 GAPS TO BE FILLED

A close relationship between histone acetylation and active gene expression is established³⁵. However, the molecular mechanism of how HATs and histone

chaperones function together to regulate histone acetylation and histone exchange during transcription is unclear. The study of chromatin regulatory proteins is a broad and complex field that is still expanding, and although our knowledge of these protein complexes has increased in recent years, there is still much to learn. Our hypothesis is chromatin is very dynamic and there are differences in eviction and acetylation kinetics during active gene transcription. In this study, we use a well-established inducible promoter to detect the impact of histone chaperones on histone occupancy and acetylation status upon gene activation. Acetylated histones H3-K9 and H3-K14 are marks often associated with transcription activation and are the key residues of our analysis. Here, we show that specific histone chaperones promote histone eviction and influence histone acetylation at inactive and active *GAL* genes *in vivo*. We also quantify the intensity of fluorescence and expression levels of GFP-histone chaperones. This should be very informative for future work on determining the sedimentation parameters of endogenous histone chaperone-HAT complexes by analytical ultracentrifugation with a fluorescence detection system.



FIGURE 1.1: DIAGRAM OF THE GAL GENES

Positions of the coding and promoter sequences for *GAL7*, *GAL10*, and *GAL1*. The amplicons used in the chromatin immunoprecipitation assays are labeled A-K.

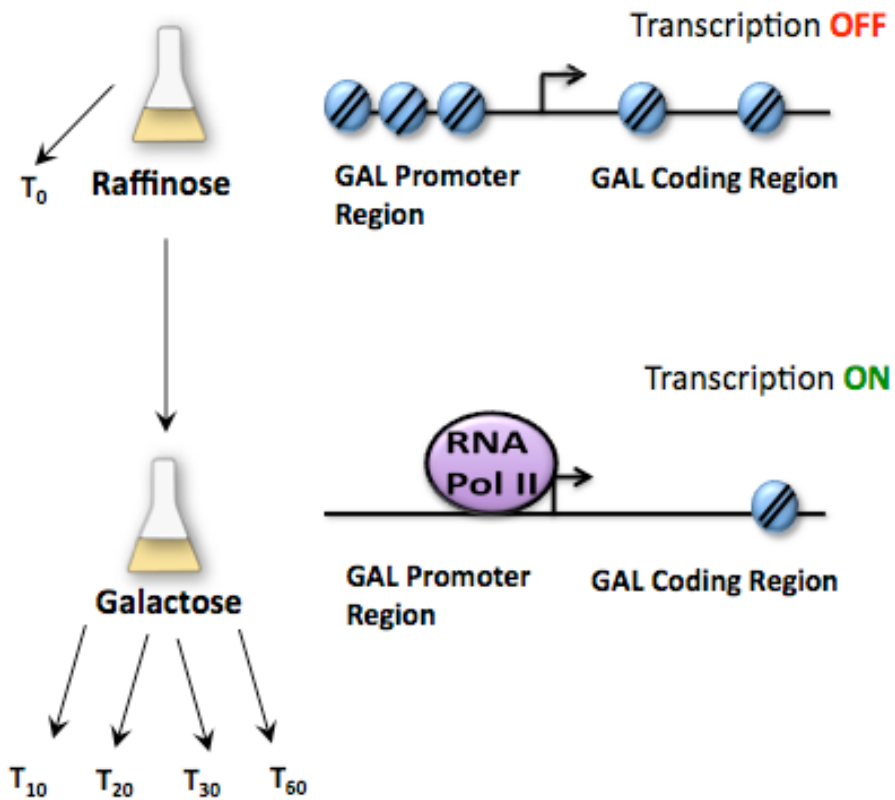


FIGURE 1.2: GALACTOSE GENE INDUCTION SYSTEM

Samples were taken after 0 (T_0), 10 (T_{10}), 20 (T_{20}), 30 (T_{30}), and 60 (T_{60}) minutes of growth in galactose. Nucleosomes are evicted from promoter and coding regions upon growth in galactose.

CHAPTER 2 MATERIALS AND METHODS

2.1 YEAST STRAINS AND MEDIA

Dr. Erin O'Shea and Dr. Jonathan Weissman at University of California-San Francisco generated the *S. cerevisiae* GFP-histone chaperone fusion proteins³⁶. The GFP fusion proteins are integrated into the yeast chromosome through homologous recombination and are expressed from endogenous promoters. The deletion mutant strains ($\Delta asf1$, $\Delta vps75$, and $\Delta nap1$) and the parental strain (BY4741) used in this study were purchased from Open Biosystems. Non-induced strains were grown in YP media containing 2% raffinose. For galactose inductions, cells were first grown in raffinose media, and then washed and transferred to YP containing 2% galactose. Cells were collected at different induction time points.

2.2 CHROMATIN IMMUNOPRECIPITATION ASSAY

Chromatin immunoprecipitation (ChIP) assays were performed as described^{37,38}. Cells (50 mL) were grown in raffinose or galactose media at 37°C to OD₆₀₀ of 0.8~1.0. Proteins were cross-linked to DNA by 1% formaldehyde for 15 minutes with gentle swirling of the media at 5-minute intervals. Glycine was added to a final concentration of 1.5M at 25°C to quench the cross-linking reaction. Chromatin was sheared by sonication using a Branson W-350 model sonifier (8 times at 8 sec each on continuous pulse at a microtip power setting of 5). Ten percent of the chromatin material used for the immunoprecipitation, which was processed as the input after reversing the cross-links and purifying the DNA. Chromatin (500 μ l) was incubated with 5 μ l of anti-H3 (Abcam), 10 μ l anti-H3K9 (Millipore), or 10 μ l anti-H3K14 (Millipore) antibodies, rotating overnight at 4°C. 50 μ l of protein-A sepharose beads was incubated with the chromatin material for 3 hours at room temperature. The beads were collected by centrifugation, and

the antigen–antibody complexes were recovered and treated with elution buffer (50 mM Tris, 10 mM EDTA, 1% SDS) for 15 minutes at 65°C to elute the complexes. Protein–DNA cross-links were reversed by incubation overnight at 65° C, and the DNA was purified by phenol–chloroform extraction and used for quantitative PCR analysis. Samples with no antibody were used as inputs. A change in the critical threshold (ΔC_T) was determined by subtracting input DNA (no IP) from the critical threshold (C_T) value measured by quantitative PCR. The protein occupancy was determined by raising the PCR efficiency to the ΔC_T value. Quantitative PCR reactions were carried out in a volume of 25 μ l using a BioRad iCycler, SYBR green fluorescein mix, and specific primers (Supplemental Table 1). Standard curves were generated using 10-fold serial dilutions of Input DNA. PCR efficiencies ranged from 90 to 100%.

2.3 WESTERN BLOT ASSAY

Yeast cells were grown in raffinose or galactose (10 ml) media to an OD_{600} of 0.8~1.0. Cells were harvested, washed with sterile water, and resuspended in 150 μ l lysis buffer (25 mM Tris Phosphate, pH 7.4 and 2 mM PMSF). Whole-cell extracts were prepared by vigorous bead beating. Cellular debris was removed by spinning the extracts at 10,000 \times g at 4° C for 15 minutes. Protein concentrations were determined by the Bradford assay (Bio-Rad). Equal concentrations (20 μ g/ μ L) of whole-cell extracts were separated on 15% SDS–PAGE and transferred to a nitrocellulose membrane. The following antibodies were used at the given dilutions: anti-H3 (Upstate, 1:1000), anti-H3K9 (Millipore, 1:5,000), anti-H3K14 (Millipore, 1:3,000), and anti-GFP (Gift from Jim Bamberg's Lab, 1:1,000)

2.4 FLUORESCENCE ASSAYS

S. cerevisiae cells expressing photo-activatable GFP-histone chaperone were grown in 10 mL of S.D. (synthetic defined) medium to an OD_{600} of 0.8~1.0. Cells were harvested, washed with sterile water, and resuspended in 150 μ l lysis buffer (25 mM Tris Phosphate, pH 7.4 and 2 mM PMSF). Whole-cell extracts were

prepared by vigorous bead beating. Cellular debris was removed by spinning the extracts at $10,000 \times g$ at $4^{\circ} C$ for 15 minutes. Protein concentrations were determined by the Bradford assay (Bio-Rad). All fluorescent assays were performed in a Horiba Jobin Yvon Fluorolog-3 spectrofluorometer. The cells were constantly stirred with a magnetic stirrer to establish uniform cell distribution during the experiment. Yeast cells were excited with 488 nm wavelength of light and peak emission wavelength intensity measured.

2.5 CELL IMAGING

S. cerevisiae cells expressing photo-activatable GFP-histone chaperone were grown in 10 mL S.D. media to an OD_{600} of 0.8~1.0. Cells were harvested and resuspended in 1 mL of 20 mM Tris-Cl pH 7.4 and 125 mM KOAc. Equal volumes (1 μ L) of yeast cells were fixed to a glass microscope slide using mounting media (9 μ L) and cover slips were sealed with nail polish. Cells containing GFP-histone chaperones were excited by 488 nm wavelengths of light. GFP-histone chaperone emission intensities were imaged and quantified using Delta Vision Personal DV Imaging System, and Z-stacks at 0.2 μ m intervals were taken through each cell.

2.6 DATA ANALYSIS

2.6.1 HISTONE H3 OCCUPANCY TABLES

The ΔC_T was determined by subtracting input DNA (no IP) from the critical threshold value (C_T) measured by quantitative PCR. The PCR efficiency determined by quantitative PCR was raised to the ΔC_T value to measure the raw histone H3 occupancy. The histone H3 occupancy was calculated by dividing the histone H3 raw occupancy values by the telomere histone H3 raw occupancy values within each sample.

$$C_T - \text{Input DNA} = \Delta C_T$$

PCR Efficiency ΔCT = Histone H3 Raw Occupancy

(EQUATION 1)

H3 Histone Occupancy =

$$\frac{\text{Histone H3 Raw Occupancy GAL Amplicon}}{\text{Histone H3 Raw Occupancy Telomere}}$$

Initial and Minimum Histone H3 Occupancy:

Normalized occupancy values were multiplied by 10

(EQUATION 2)

Time Independent Fold Eviction =

$$\frac{\text{Initial H3 Occupancy } T_0}{\text{Minimum H3 Occupancy Observed}}$$

(EQUATION 3)

Time Dependent Fold Eviction T_{20} =

$$\frac{\text{Initial Occupancy } T_0}{\text{Histone Occupancy } T_{20}}$$

(EQUATION 4)

Time Dependent Fold Eviction T_{30} =

$$\frac{\text{Initial Occupancy @ } T_0}{\text{Histone Occupancy @ } T_{30}}$$

(EQUATION 5)

Histone H3 Eviction Rate =

$$\frac{\text{Initial Histone Occupancy} - \text{Minimum Histone Occupancy}}{T_{\text{Minimum Histone Occupancy}}}$$

*Normalized eviction rate values were multiplied by 10

Time at Which Half Histone H3 Eviction Occurs (T_0 Dependent)

Maximum histone occupancy values observed at T_0 (raffinose) were set to 100 and additional time points were normalized to this value. The time at which half of the maximum eviction occurred was determined by graphing the adjusted acetylation occupancy values versus time. A tangent line was extrapolated from the half eviction level down to the time at which it occurred.

2.6.2 Histone Acetylation Tables

The ΔC_T was determined by subtracting input DNA (no IP) from the critical threshold value (C_T) measured by quantitative PCR. The PCR efficiency determined by quantitative PCR was raised to the ΔC_T value to measure the raw histone H3 acetylation. The histone H3 acetylation (K9 and K14) values were calculated by dividing the histone H3 raw acetylation values by the telomere histone H3 raw acetylation values within each sample.

$$C_T - \text{Input DNA} = \Delta C_T$$

$$\text{PCR Efficiency}^{\Delta C_T} = \text{K9 (K14) Raw Acetylation}$$

(EQUATION 6)

H3 Histone Acetylation =

$$\frac{\text{Raw K9 (K14) Acetylation GAL Amplicon} / \text{Raw K9 (K14) Acetylation Telomere}}{\text{H3 Occupancy GAL Amplicon} / \text{H3 Occupancy Telomere}}$$

Initial and Maximum Histone H3-K9/H3 and H3-K14/H3 Histone Acetylation (T_0)

*Normalized histone acetylation levels were multiplied by 10

(EQUATION 7)

$$\text{Time Independent Fold Acetylation} = \frac{\text{Maximum Acetylation Observed}}{\text{Initial Acetylation}}$$

(EQUATION 8)

$$\text{Time Dependent Histone H3 (K9/H3 and K14/H3) Fold Acetylation } T_{20} = \frac{\text{Acetylation Value } T_{20}}{\text{Initial Acetylation}}$$

(Equation 9)

$$\text{Time Dependent Histone H3 (K9/H3 K14/H3) Fold Acetylation } T_{30} = \frac{\text{Acetylation } T_{30}}{\text{Initial Acetylation}}$$

(Equation 10)

$$\text{Histone H3-K9/H3 and H3-K14/H3 Acetylation Rate} = \frac{\text{Maximum Acetylation-Initial Acetylation}}{T_{\text{Maximum Acetylation}}}$$

Time at Which Half Histone H3 Acetylation (H3-K9/H3 and H3-K14/H3) Occurs

The maximum acetylation value observed was set to 100 and additional time points were normalized to this value. The time at which half of the maximum acetylation occurred was determined by graphing the adjusted acetylation occupancy values versus time. A tangent line was extrapolated from the half eviction level down to the time at which it occurred.

CHAPTER 3 HISTONE EVICTION AND MODIFICATIONS AT GALACTOSE INDUCIBLE GENES

3.1 ABSTRACT

In eukaryotes, the genome is organized in DNA and histones to form chromatin. The highly compact nature of chromatin creates a barrier for proteins that require access to DNA during replication, transcription, and DNA repair. During transcription activation, histones are exchanged from promoter and coding regions to allow efficient synthesis of mRNA. Additionally, histone acetylation is correlated with active gene transcription. Here, we characterize location-specific effects of histone eviction and histone acetylation at galactose inducible genes *in vivo* across time. Our approach is highly sensitive allowing for the determination of histone H3 occupancy and acetylation status of key lysine residues on histone tails at promoter and coding regions upon gene activation. We show that there are significant location specific effects in regard to histone H3 eviction and acetylation at promoter and coding regions at galactose inducible genes.

3.2 INTRODUCTION

The basic level of organization of chromatin is a histone octamer (two of each histone H2A, H2B, H3, and H4), which organizes 147 base pairs of DNA in two super-helical turns to create the nucleosome core particle ¹. Remodeling of chromatin plays a key role in the regulation of gene expression through histone modifying activities. Histones are acetylated and evicted from promoter regions upon transcription activation to allow binding of the pre-initiation complex. Additionally, nucleosomes are evicted from coding regions to allow passage of RNA polymerase II. However, it is unclear if regions within the genome contain varying amounts of histone occupancy and acetylation kinetics that occur upon gene activation, and to what extent. Furthermore, it is unknown to what degree these histone modifications are altered upon gene activation. Here, we use a

well-studied gene expression system to study these types of location specific effects of promoter and coding regions. We hypothesize that there will be significant differences in histone H3 eviction profiles and acetylation status at promoter and coding regions. More specifically, we expect to see decreased amounts of histone H3 acetylation at promoter regions compared to coding regions due to the fact that active promoter regions need to be highly accessible to transcription factors. The *GAL* genes are an ideal system to study changes in nucleosome occupancy and acetylation upon gene activation because nucleosomes are evicted from promoter and coding regions during growth in galactose³⁹. We show that promoter and coding regions contain different densities of nucleosomes with varying degrees of histone acetylation that contribute to different eviction profiles and acetylation rates at the galactose inducible genes *in vivo*.

3.3 RESULTS

Transcription by RNA polymerase II on a chromatin template is accompanied by dynamic changes in the chromatin structure, such as the eviction or post-translational modifications of histones. To understand histone mobility and the role of acetylation at the galactose inducible genes, chromatin immunoprecipitation (ChIP) assays were used to map the occupancy of histone H3 and the levels of acetylated histones (H3-K9/H3 and H3-K14/H3).

PROMOTER REGIONS CONTAIN DECREASED LEVELS OF HISTONE H3 AT INACTIVE *GAL* GENES

First, we wanted to determine the amount of histone H3 present at the *GAL* genes during repressive conditions (growth in raffinose). Histone H3 was cross-linked to various promoter and coding regions within the *GAL* genes, which allowed the comparison of location-specific variations of histone occupancy. With this system, the galactose-inducible genes were analyzed by changing the medium from raffinose (off) to galactose (on). In repressive conditions, we observed that histone H3 density is comparable across the 3' end of coding

regions at the *GAL7*, *1*, *10* genes (Fig. 3.1). Histone H3 normalized occupancy (See equation 1 in Materials and Methods for normalization description) for these coding regions ranged from 1.5 to 2.0. We observed a slight decrease in H3 occupancy at the 5' end of coding regions of *GAL10* and *GAL7*. As expected, there is decreased histone H3 occupancy at promoter regions compared to coding regions. Promoter regions at the *GAL* genes contained histone H3 occupancy levels of 1.0. The *GAL1*, *10* and *GAL 7* UAS and TATA boxes showed a 2-fold decrease in histone H3 occupancy when compared to the occupancy found at *GAL1* and *GAL10* coding regions.

HISTONE H3 IS EVICTED FROM PROMOTER AND CODING REGIONS UPON TRANSCRIPTION ACTIVATION

Next, we wanted to characterize H3 eviction patterns seen within activate *GAL* genes and uncover any location specific differences in H3 eviction parameters (rate and fold eviction). Upon galactose induction, histones are evicted from promoter and coding regions to allow the binding and passage of RNA polymerase II (Fig. 3.2). We observed that the majority of coding regions contain greater occupancy of histone H3 than promoter regions during activating conditions (10, 20, 30, and 60 minutes of growth in galactose) (Fig 3.3). The histone H3 occupancy difference observed between promoter and coding regions became more obvious throughout the galactose time course. Thus, promoter regions contain less histone H3 than coding regions at active and inactive *GAL* genes.

We observed different histone H3 occupancy at amplicons A-K throughout the galactose time course that contribute to different eviction profiles and H3 eviction rates for the various amplicons (Supplemental Table 2). However, even though the rate and fold eviction varies across the *GAL* locus, histone H3 evicts to similar levels at the end of the galactose time course at every amplicon. After 60 minutes of growth in galactose, amplicons H3 occupancy ranged from 0.05 to 0.4.

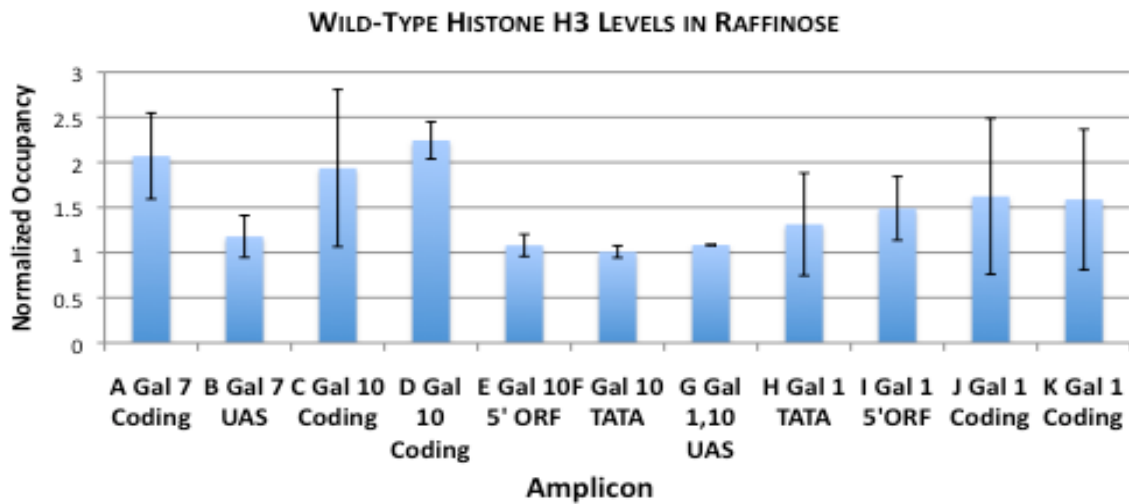


FIGURE 3.1: WILD-TYPE PROMOTER REGIONS CONTAIN DECREASED LEVELS OF HISTONE H3 OCCUPANCY COMPARED TO CODING REGIONS AT GAL GENES

ChIP analysis of histone H3 were performed in raffinose (T_0). Each column corresponds to the location of a real-time PCR amplicon. Error bars indicate standard deviations from two independent biological replicates and are normalized to a telomere control.

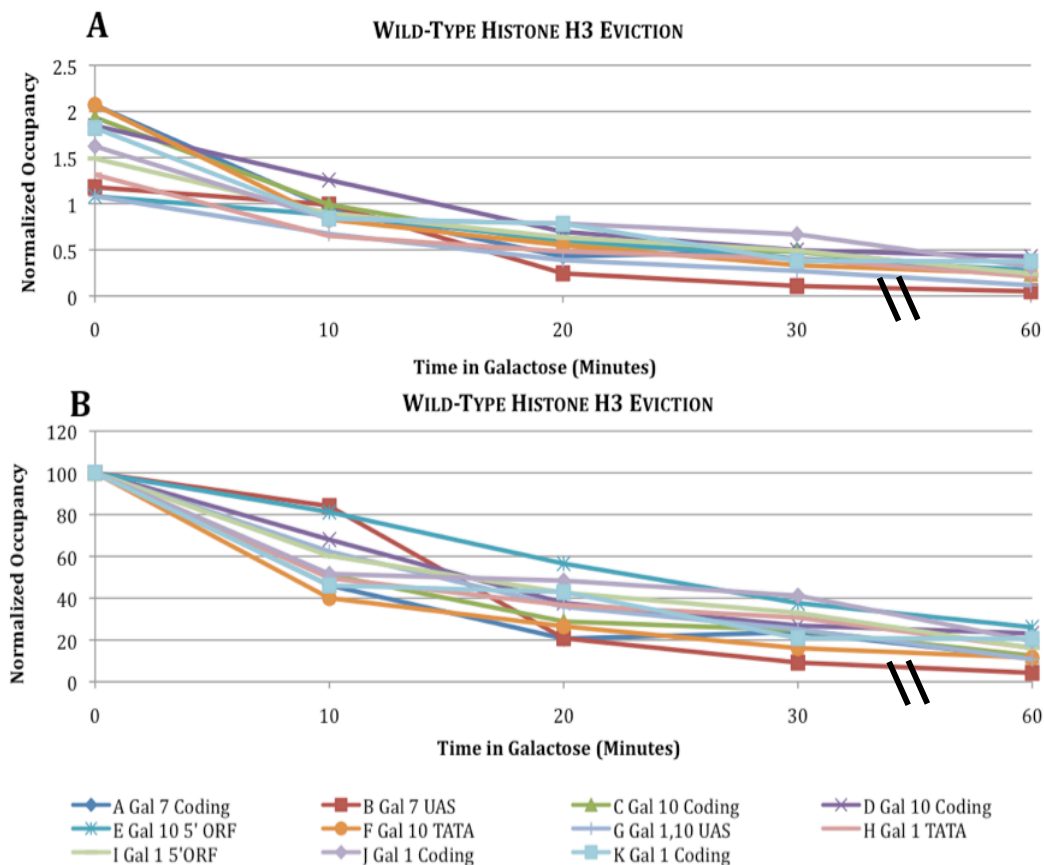


FIGURE 3.2: HISTONE H3 IS EVICTED FROM PROMOTER AND CODING REGIONS UPON TRANSCRIPTION ACTIVATION

ChIP analyses of histone H3 at galactose inducible promoters and coding regions were performed in raffinose (T_0) or galactose (T_{10} T_{20} T_{30} T_{60}). **(A)** Normalized histone H3 occupancy **(B)** Initial normalized histone H3 occupancy (T_0) was set to 100 and additional time points were adjusted to this value. Each study was performed in biological duplicate, and normalized to a telomere control. Hatch marks indicate non-linear time on the x-axis.

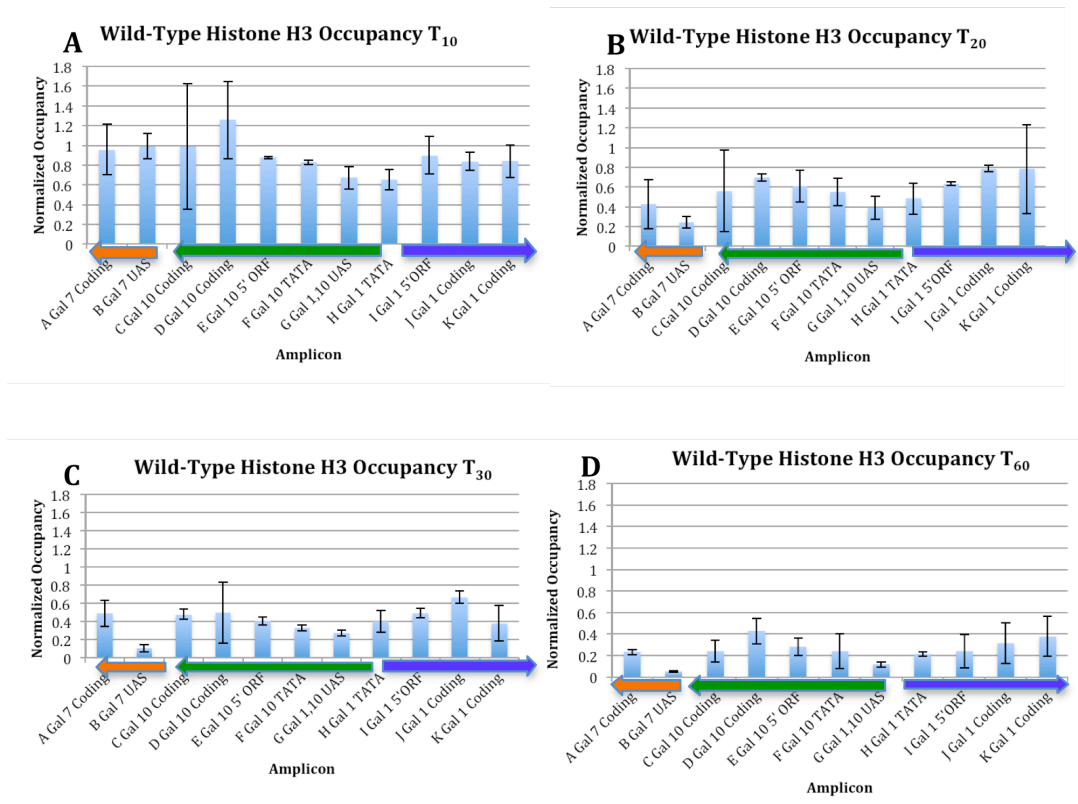


FIGURE 3.3: THE GAL GENE PROMOTERS HAVE DECREASED LEVELS OF HISTONE H3 OCCUPANCY DURING ACTIVATING CONDITIONS

ChIP analyses of histone H3 occupancy at galactose inducible promoters and coding regions were performed after growth in galactose media for (A) 10 minutes T₁₀ (B) 20 minutes T₂₀ (C) 30 minutes T₃₀ (D) 60 minutes T₆₀ at amplicons A-K. Each study was performed in duplicate, and normalized to a telomere control. Hatch marks indicate non-linear time on the x-axis.

THE *GAL* GENES HAVE DIFFERENT HISTONE H3 EVICTION PROFILES

We showed that cells grown in raffinose have histone H3 levels that are comparable to coding regions while there is decreased histone H3 occupancy at promoter regions. Next, we wanted to determine if there were differences in the eviction profiles of amplicons spanning the *GAL* genes (Fig.3.4). Eviction profiles describe histone H3 occupancy over time during growth in galactose containing media. Indeed, we observed different degrees of histone H3 eviction at the *GAL* genes. Most coding regions initially have 2 units of histone H3 while promoter regions and the *GAL* 5' ORF had between 1 and 1.5 units during growth in raffinose. After 10 minutes of galactose induction, we observed all amplicons were able to evict to 1 unit of histone H3 or less. The first 10 minutes of galactose induction appears to be the time at which the most histone H3 is evicted from *GAL* genes. However, this is not true at the *GAL7* UAS and the *GAL10* 5' ORF where there is almost no H3 eviction the first 10 minutes of growth in galactose. At the *GAL7* UAS, histone H3 evicts the most between 10 minutes and 20 minutes reaching eviction levels close to zero. The majority of the other amplicons that have histone H3 occupancy of 1 unit at 10 minutes and take 60 minutes of growth in galactose to evict to zero. Interestingly, we do not observe a similar histone H3 eviction profile for the *GAL7* UAS and the *GAL1, 10* UAS. At the *GAL1, 10* UAS histone H3 evicts to a greater extent during 0-10 minutes of growth in galactose and takes longer (30 minutes) to reach eviction levels found at the *GAL7* UAS.

HISTONE H3 EVICTION RATE IS INVERSELY PROPORTIONAL TO TIME IN GALACTOSE

We calculated the rate of histone H3 eviction at promoter and coding regions upon galactose induction using the above data (see equation 5 in Materials and Methods Chapter for eviction rate description). Eviction rate was calculated for absolute eviction (Initial Occupancy-Lowest Occupancy / Time) and during 0-10 minutes (Initial Occupancy- Occupancy T_{10} / 10 minutes), 10-20 minutes (Occupancy T_{10} - Occupancy T_{20} / 10 minutes), 20- 30 minutes (Occupancy T_{20} - Occupancy T_{30} / 10 minutes), and 30-60 (Occupancy T_{30} - Occupancy T_{60} / 30

minutes) minutes of galactose induction (Fig. 3.5). During the initial 10 minutes of galactose induction, we observed eviction rates between 1-2 histone H3 per minute evicted. During 10-20 minutes of galactose induction, we observed a decrease in eviction rate ranging from 0.5-1.2 histone H3 per minute evicted. During 20-30 minutes of galactose induction, we saw another decrease in histone H3 eviction across the *GAL* genes with the maximum rate of H3 eviction being 0.7 histone H3 per minute evicted. Finally, between 30 and 60 minutes of galactose induction the rate of H3 eviction continued to decrease at the majority of amplicons ranging from 0.1-0.7 histone H3 per minute. Interestingly, we observed decrease rates of histone H3 eviction occurring at the *GAL7* and *GAL1*, 10 UAS and 5' promoter regions whereas coding regions eviction rates tended to be higher.

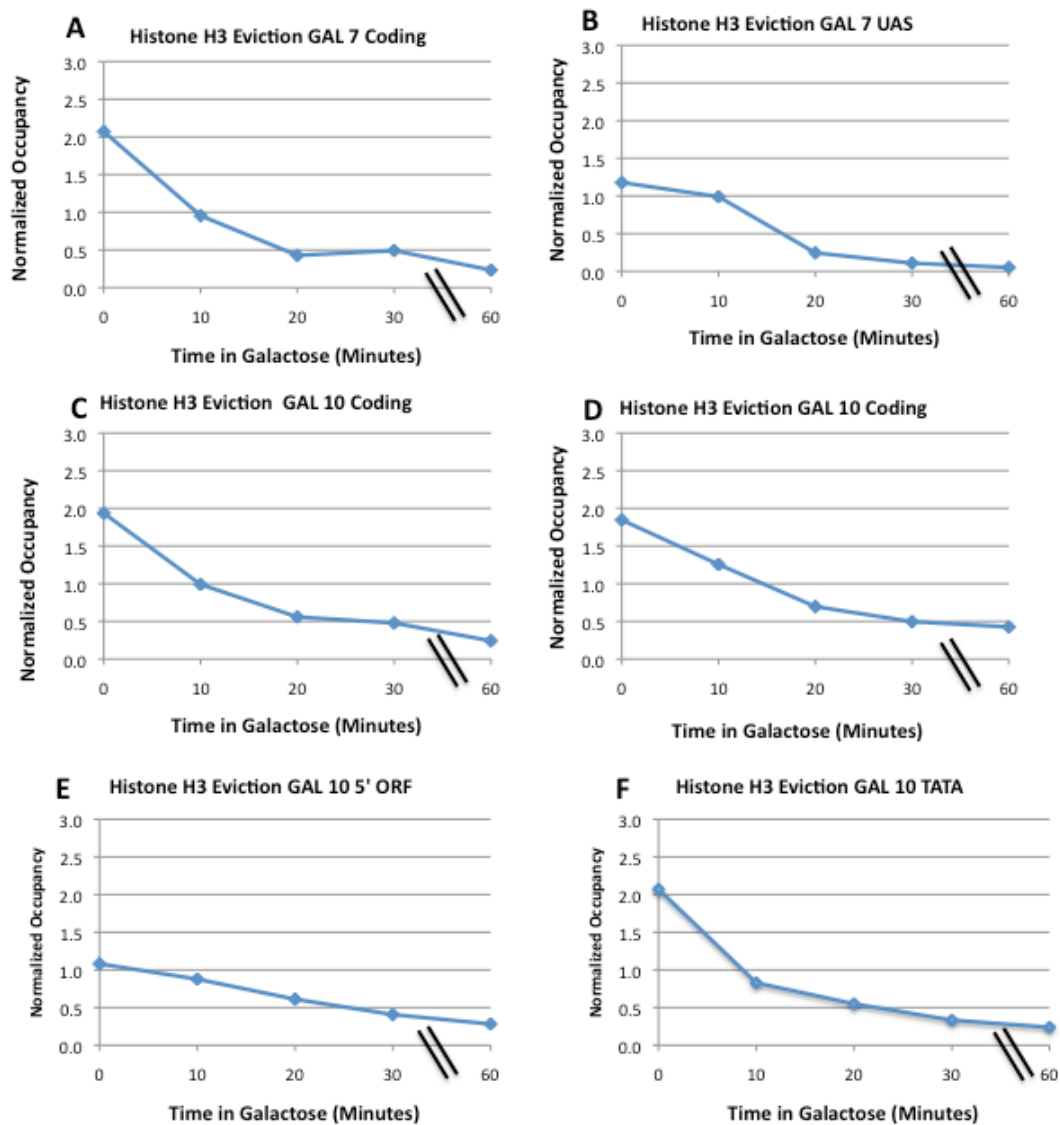


FIGURE 3.4: PROMOTER AND CODING REGIONS WITHIN THE GAL GENES HAVE DIFFERENT HISTONE H3 EVICTION PROFILES

ChIP analyses of histone H3 at galactose inducible promoters and coding regions were performed in raffinose (T_0) or galactose (T_{10} , T_{20} , T_{30} , T_{60}) at amplicons A-K. Each study was performed in duplicate, and normalized to a telomere control. Hatch marks indicate non-linear time on the x-axis.

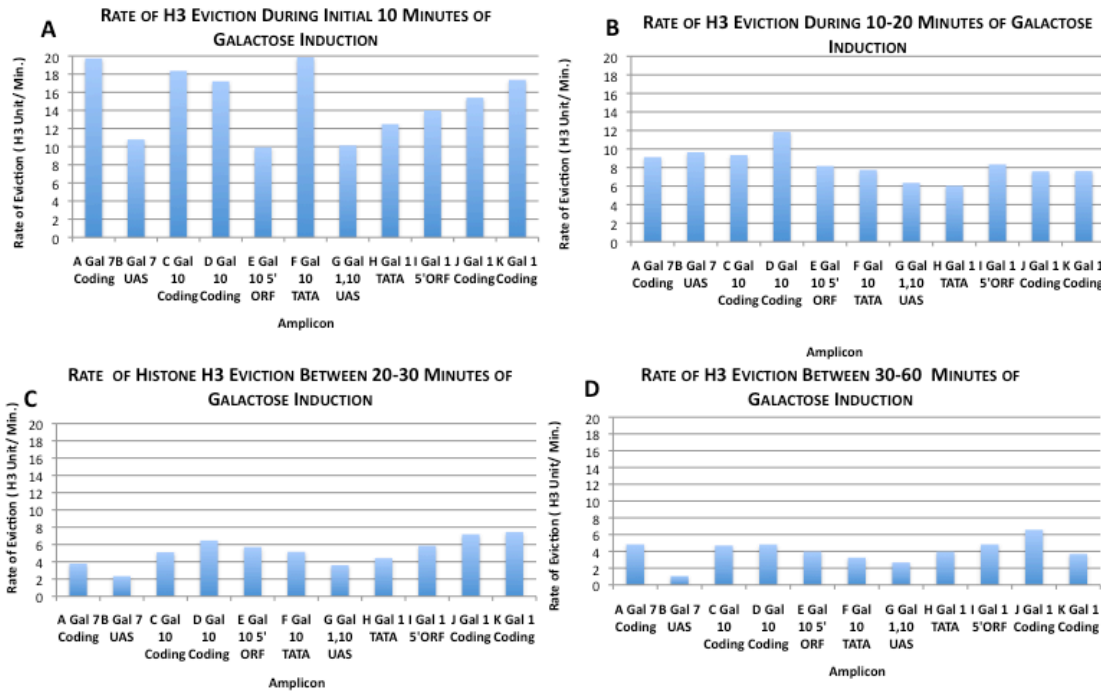


FIGURE 3.5: HISTONE H3 EVICTION RATE DECREASES WITH TIME IN GALACTOSE

Histone H3 eviction rate (multiplied by 10) was calculated between (A) 0-10 minutes, (B) 10-20 minutes, (C) 20-30 minutes, and (D) 30-60 minutes from normalized CHIP values.

PROMOTER REGIONS CONTAIN INCREASED LEVELS OF ACETYLATION DURING LATE TRANSCRIPTION

Acetylation of the histone H3-K14 and H3-K9 by HATs is generally correlated with transcriptional activation. We wanted to determine the amounts of histone H3-K9/H3 and H3-K14/H3 acetylation at the *GAL* locus before and after gene activation. Before we examined acetylation levels during transcription, we first wanted to examine the levels of H3-K9/H3 prior to transcription activation. The amount of H3-K9/H3 acetylation was similar at all amplicons (A-K) during repressive conditions (Fig. 3.6A). We observed acetylation values ranging from 0.8-1.6. Upon transcription activation with the addition of galactose media, we observed an increase in H3-K9/H3 acetylation at amplicons A-K that positively correlated with time in galactose. After 10 minutes of growth in galactose, histone H3-K9/H3 acetylation levels were similar except the *GAL7* UAS, which was 2-fold higher than the majority of amplicons (Fig. 3.7A). After 20 minutes of growth in galactose, we observed decreased acetylation at the 3' end and increased acetylation at promoter regions and the 5' end of *GAL* genes. This trend of peak acetylation at promoter regions and 5' end of genes is maintained through 30 and 60 minutes of growth in galactose. After 60 minutes of induction, acetylation levels at promoter regions are significantly higher than coding regions at *GAL1*, *10*, and *7*. The greatest difference in H3-K9/H3 acetylation between promoter and coding regions was observed at *GAL7* (3-fold difference).

We observed similar levels of histone H3-K14 acetylation at amplicons A-K during repressive conditions (Fig. 3.6 B). Next, we wanted to test location specific differences in the amount of H3-K14 acetylation at specific time points throughout galactose induction (Fig. 3.7 B). After 10 minutes of galactose induction, we see similar amounts of H3-K14/H3 acetylation at promoter and coding regions. After 20 minutes of growth in galactose, we see decreased levels H3-K14/H3 acetylation at the outer amplicons (*GAL7* ORF and *GAL1* ORF). Interestingly after 30 and 60 minutes of growth in galactose, we see this similar trend as histone H3-K9/H3 acetylation were the 5' end of the *GAL* genes contain increased acetylation when compared to the 3' end.

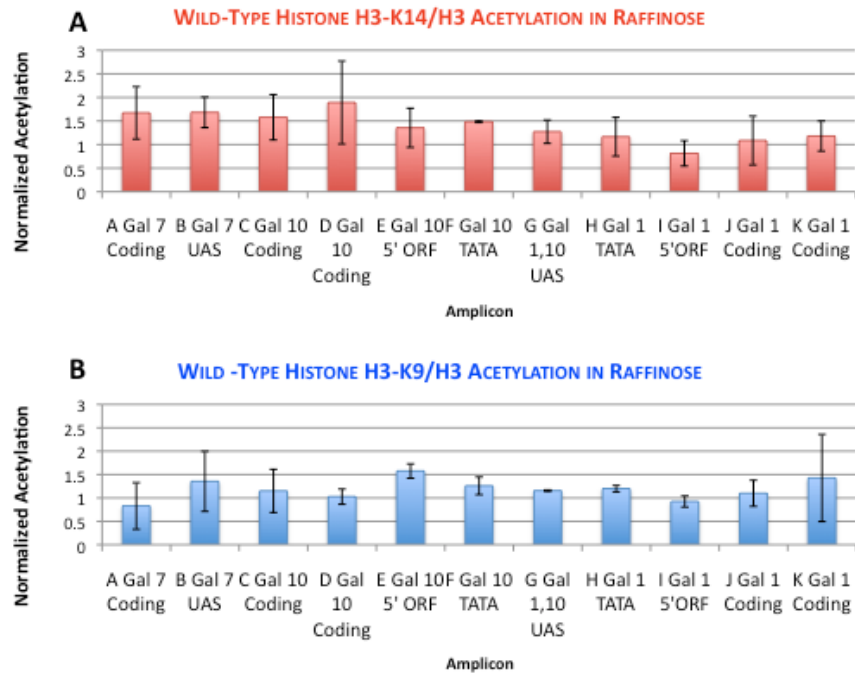


FIGURE 3.6: WILD-TYPE CELLS CONTAIN SIMILAR LEVELS OF HISTONE H3-K9 AND H3-K14 ACETYLATION AT GAL GENES

ChIP analyses of acetylated histones (A) H3-K14/H3 and (B) H3-K9/H3 were performed on wild-type cells. Each column corresponds to the location of a real-time PCR amplicon. Error bars indicate standard deviations from two independent biological replicates.

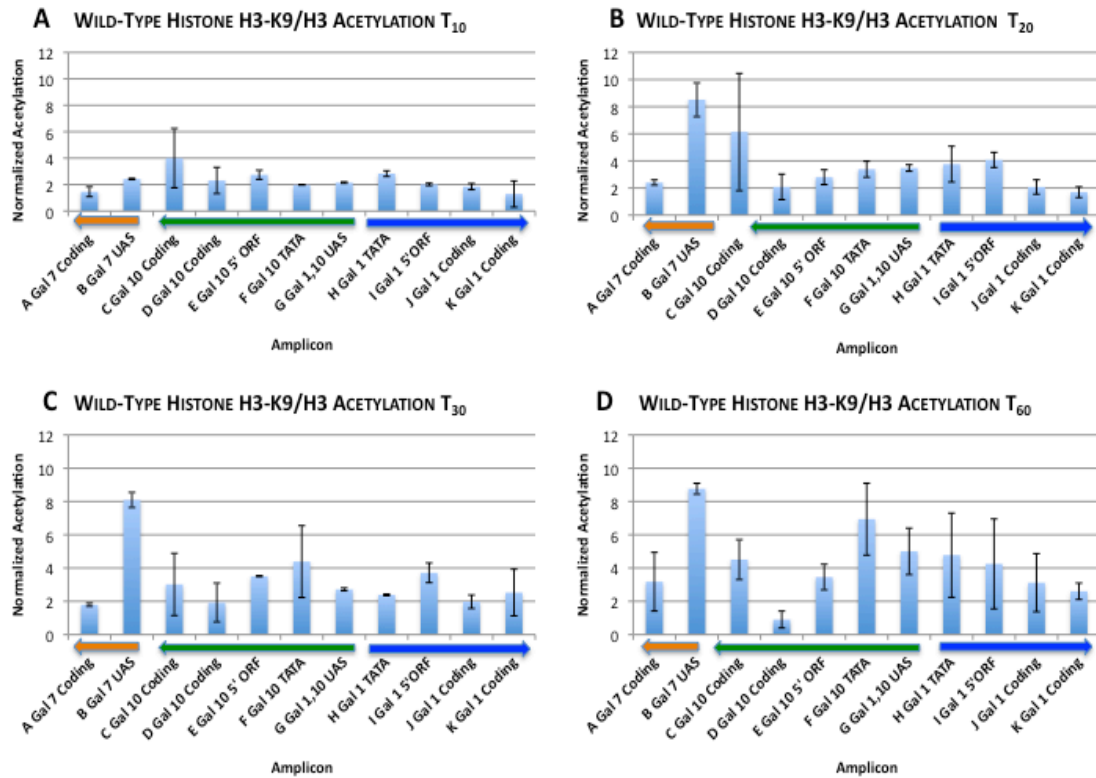


FIGURE 3.7: PROMOTER REGIONS CONTAIN INCREASED LEVELS OF HISTONE ACETYLATION AT ACTIVE *GAL* GENES

ChIP analyses of histone H3-K9/H3 acetylation at *GAL* genes were after (A) 10 minutes T_{10} (B) 20 minutes T_{20} (C) 30 minutes T_{30} (D) 60 minutes T_{60} minutes of growth in galactose medium. Each study was performed in duplicate, and normalized to a telomere control. Error bars indicate standard deviations from 2 independent biological replicates.

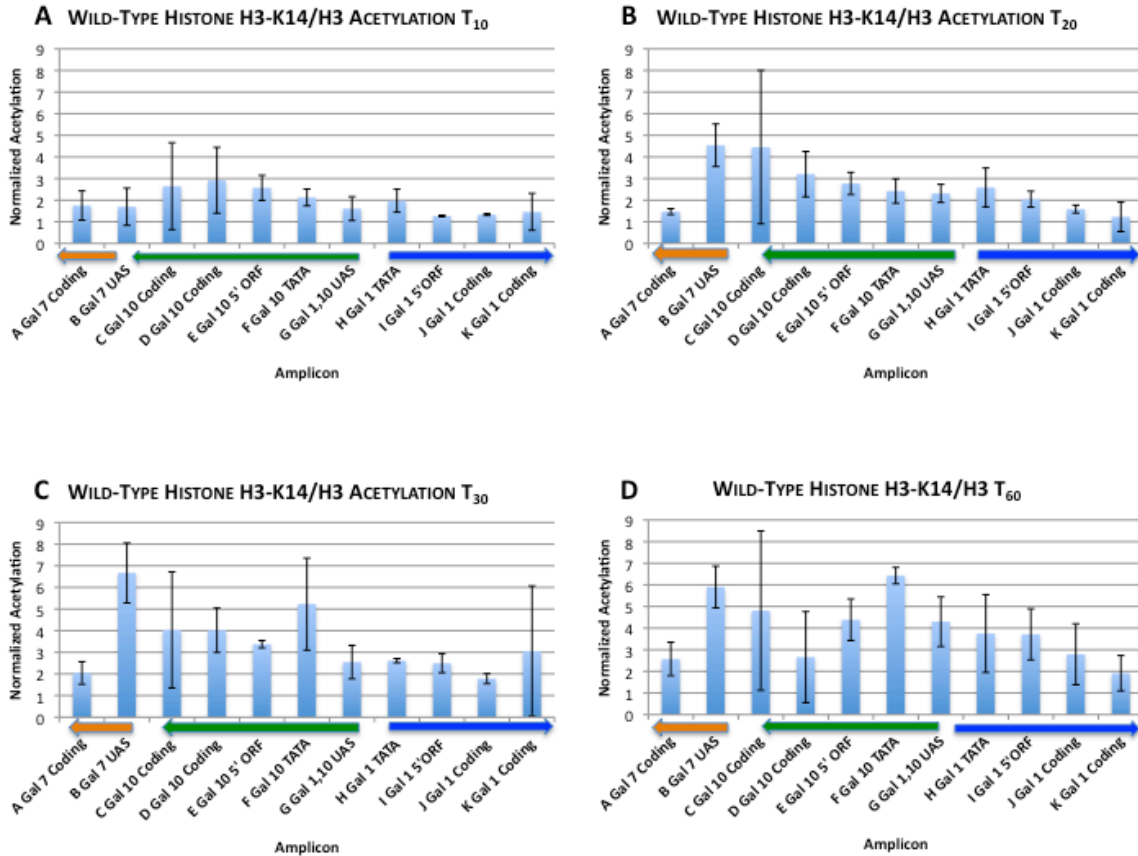


FIGURE 3.8: PROMOTER REGIONS CONTAIN INCREASED LEVELS OF HISTONE H3 ACETYLATION AT ACTIVE GAL GENES

ChIP analyses of histone H3-K14/H3 acetylation at *GAL* genes were after (A) 10 minutes T₁₀ (B) 20 minutes T₂₀ (C) 30 minutes T₃₀ (D) 60 minutes T₆₀ minutes of growth in galactose medium. Each study was performed in duplicate, and normalized to a telomere control. Error bars indicate standard deviations from 2 independent biological replicates.

PROMOTER REGIONS CONTAIN INCREASED LEVELS OF ACETYLATION AT *GAL* GENES

Fold acetylation varied at different amplicons across the *GAL* genes as well (Supplemental Table 6-8). Fold acetylation is defined as the maximum amount of acetylation that occurred during the galactose time course divided by the initial acetylation (T_0) (Equation 2 in Materials and Methods Chapter). We observed an increase in absolute fold acetylation (H3-K14/H3 and H3-K9/H3) at promoter regions when compared to coding regions at the *GAL* genes (Fig. 3.8). At the *GAL1* and *GAL7* genes, the UAS exhibited a greater fold H3 acetylation than their coding regions. Similarly, the *GAL10* TATA box exhibited greater fold acetylation than its coding region. Furthermore, we observed differences in absolute acetylation rate at different amplicons. Acetylation rate (See equations 7-10 for histone H3 acetylation rates in Material and Methods Chapter) was calculated for absolute acetylation (Maximum Acetylation-Initial Acetylation/ Time of Maximum Acetylation) and during 0-10 minutes (Initial Acetylation- Acetylation T_{10} / 10 minutes), 10-20 minutes (Acetylation T_{10} - Acetylation T_{20} / 10 minutes), 20- 30 minutes (Acetylation T_{20} - Acetylation T_{30} / 10 minutes), and 30-60 (Acetylation T_{30} - Acetylation T_{60} / 30 minutes) minutes of galactose induction (Fig. 3.9). A negative acetylation rate value means that the level of acetylation decreased during that time period. We observed that the rate of acetylation decreased throughout the galactose time course. During initial galactose induction, we see a increased acetylation rate of histone H3-K9 compared to that of histone H3-K14. Additionally, acetylation appears to be more concentrated at the inner locations at each *GAL* gene with decreased acetylation at outer *GAL* genes locations. During 10-20 minutes of galactose induction, acetylation rates are similar with the exception of H3-K9 and H3-K14 acetylation rates are greater at the *GAL7* UAS. Interestingly, we observed spikes of H3-K14/H3 acetylation rate during 20-30 minutes of galactose induction. Between 30-60 minutes of galactose induction there were very low levels of both K9/H3 and K14/H3 acetylation across the *GAL* locus. The greatest difference in acetylation rates was observed at the two UAS (*GAL7* and *GAL1*, 10). The *GAL7* UAS exhibited faster absolute acetylation rates for histone H3-K9/H3 and H3-K14/H3 than the

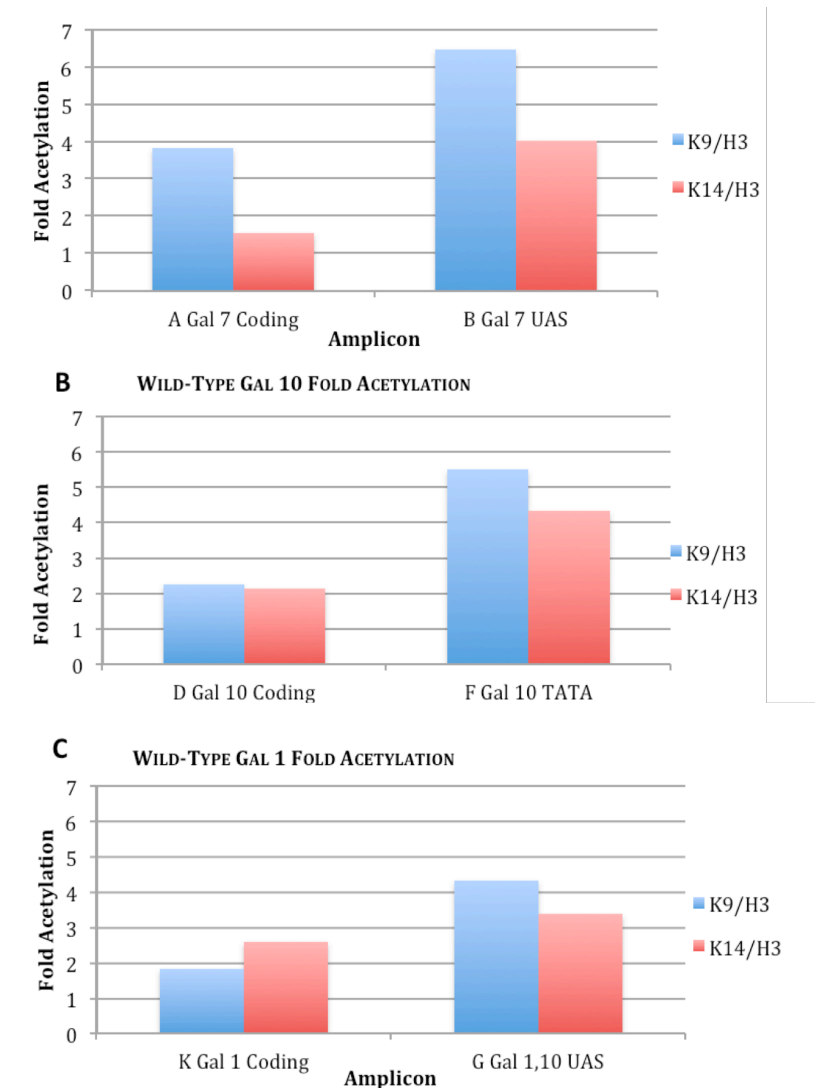


FIGURE 3.8: WILD-TYPE PROMOTER REGIONS CONTAIN INCREASED LEVELS OF FOLD HISTONE H3 ACETYLATION
 ChIP analyses of histone H3-K9 and H3-K14 acetylation at galactose inducible promoters and coding regions were performed in raffinose (T_0) or galactose (T_{10} , T_{20} , T_{30} , T_{60}). Fold acetylation rates were calculated using normalized ChIP data.

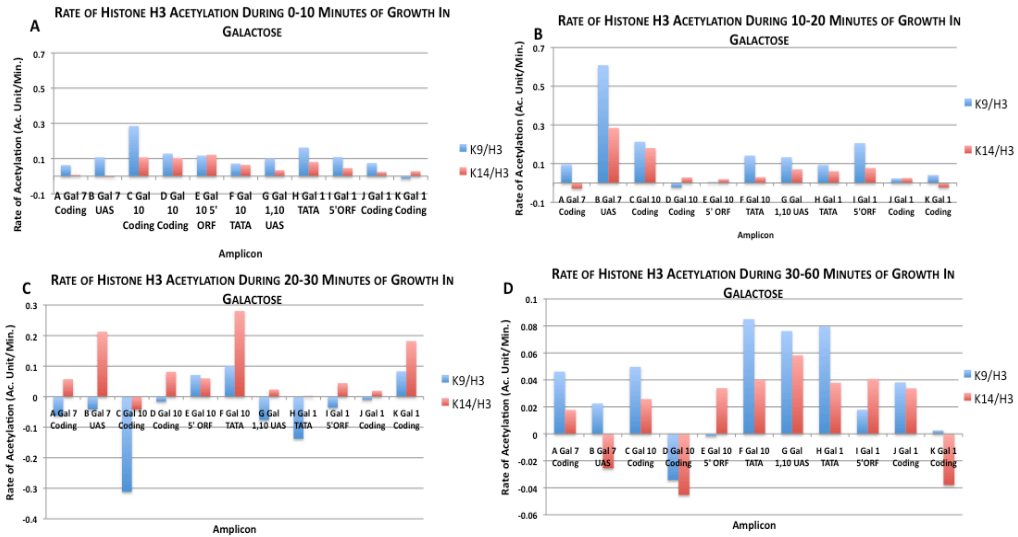


FIGURE 3.9 HISTONE ACETYLATION RATE DECREASES ACROSS THE GAL GENES WITH TIME IN GALACTOSE

Histone H3 acetylation rates (H3-K9 and H3-K14) were calculated between (A) 0-10 minutes, (B) 10-20 minutes, (C) 20-30 minutes and (D) 30-60 minutes using normalized ChIP acetylation values.

WILD-TYPE HISTONE H3 ABSOLUTE ACETYLATION RATE

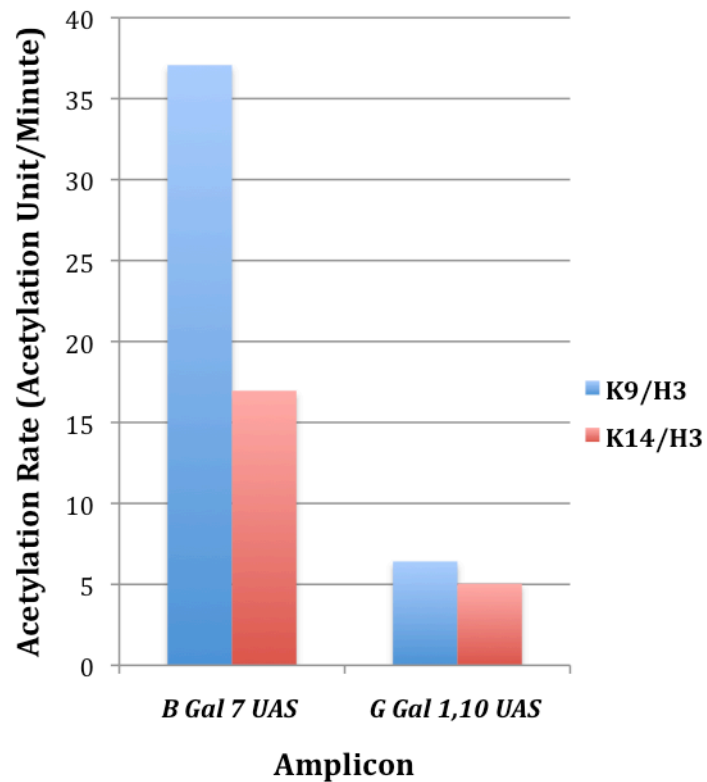


FIGURE 3.10: THE *GAL7* UAS HAS A HIGHER HISTONE H3 ACETYLATION RATE THAN THE *GAL1, 10* UAS

Acetylation rate was determined by subtracting initial normalized acetylation values (T_0) from the maximum normalized acetylation value and divided by the time it took for this maximum acetylation to occur during the galactose time course. Histone acetylation rate were calculated from normalized ChIP values.

GAL1, 10 UAS (Fig. 3.10). More specifically, the *GAL7 UAS* had a 7-fold higher acetylation rate of H3-K9/H3 and a 3-fold higher H3-K14/H3 acetylation rate than the *GAL1, 10 UAS*.

3.4 Discussion

Histone mobilization and histone acetylation have long been associated with active gene expression³⁵. However, the extent of nucleosome disassembly and acetylation at the *GAL* genes has yet to be characterized. Here we show that there are varying amounts of histone eviction and acetylation found at different regions of the *GAL* genes. We hypothesized that the chromatin architecture found at promoter regions would be more open and accessible to chromatin remodeling factors and transcription machinery than coding regions. Thus, we expected to find decreased amounts nucleosomes (H3) and increased acetylation present at promoter regions, two characteristics of accessible chromatin. Furthermore, since acetylated nucleosomes must be evicted from promoter and coding regions upon gene induction, we hypothesized that the *GAL* genes would contain increased acetylation with increased growth in galactose. First, we determined the initial histone H3 occupancy found at promoter and coding regions during growth in raffinose across the *GAL* locus (Fig 3.11A). As expected, we observed that promoter regions such as the UAS and TATA boxes contain decreased amounts of nucleosomes compared to coding regions. The UAS has been reported to contain nucleosome free regions and is a binding site for proteins that may compete with binding of nucleosomes. Interestingly, we also saw lower histone H3 levels at a 5' coding region. We believe that the nucleosomes present at promoter regions are very tightly positioned whereas at coding regions they are more randomly placed. The decreased amounts of well-positioned nucleosomes found at promoter regions makes these regions more accessible to DNA binding proteins. Promoter regions that contain less nucleosome at inactive genes are a plausible mechanism as to how transcription could be activated more efficiently. Transcription is a highly dynamic process that needs to be turned on and off very rapidly. By having a similar chromatin

environment (decreased nucleosomes) at inactive genes and active promoter regions makes the transition to active transcription less complex.

Upon growth in galactose, we observed that histones were evicted from promoter and coding regions (3.11 B). However, at each amplicon histone H3 was evicted to different levels and at different rates throughout the time course. We observed decreased amounts of H3 at active promoters compared to active coding regions. The *GAL7* UAS, *GAL1*, *10* UAS, *GAL10* and *GAL1* TATA boxes all contained depleted levels of histone H3 when compared to their respected coding regions at active *GAL* genes. We observed that not only do promoter regions have decreased levels of H3 during active conditions; promoters exhibit decreased histone H3 eviction rates when compared to coding regions. This is most likely due to the fact that promoters bear less H3 to begin with and they do not need to evict at the rate of coding regions, which have more H3 to evict upon activating conditions.

Next, we determined that there are similar amounts of histone acetylation (H3-K9/H3 and H3-K14/H3) at inactive *GAL* genes (Fig. 3.11A). Upon transcription activation we noticed location specific differences in acetylation profiles at coding and promoter regions (Fig. 3.11B). There are increased levels of acetylation (H3-K9/H3 and H3-K14/H3) at promoter regions compared to coding regions at active *GAL* genes. The increased acetylation seen at promoter regions likely causes these regions to be more relaxed and open.

Taken together, we observed fewer nucleosomes present at promoter regions that evict slower than those in coding regions at active genes. Additionally, the lower levels of histone H3 present at promoter regions are hyper-acetylated compared those at coding regions at active *GAL* genes. These differences between acetylation and eviction that we see at promoter and coding regions explain how promoter regions and regions close to the promoter seem to create a more ideal environment (less compacted) for transcription to be initiated.

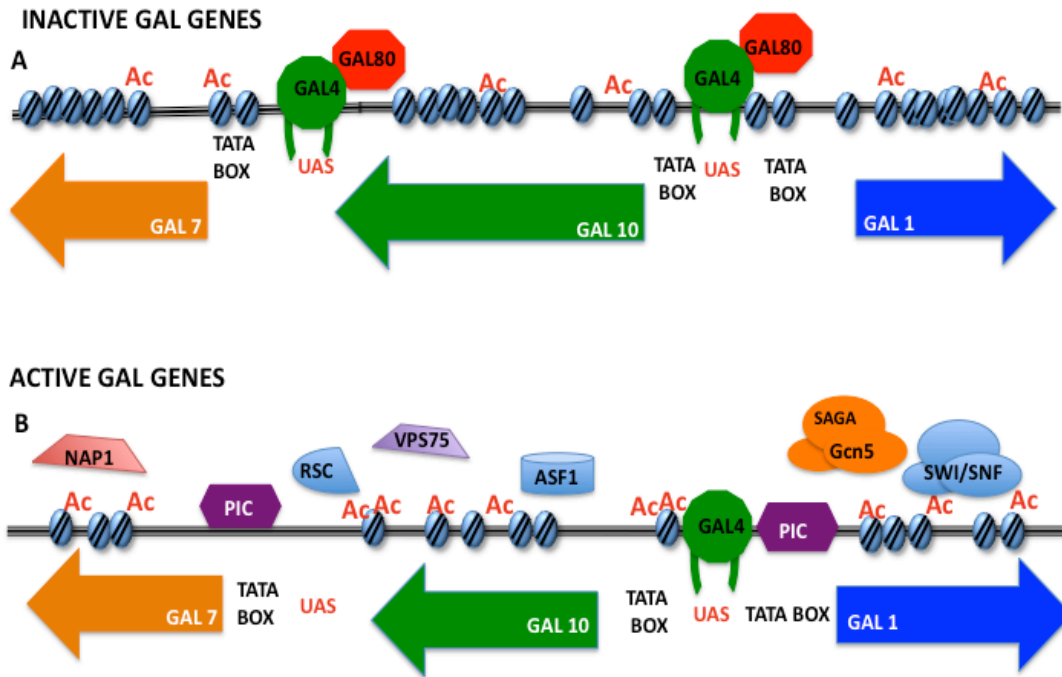


FIGURE 3.11: PROMOTER REGIONS CONTAIN INCREASED NUCLEOSOMES THAT ARE HIGHLY ACETYLATED DURING ACTIVATING CONDITIONS AT GAL GENES

(A) During transcription repression, at the *GAL* genes there is decreased density of nucleosomes found at promoter regions. Histone acetylation levels (H3-K9/H3 and H3-K14/H3) are low but comparable across amplicons. The repressor, Gal80, is bound to the active site of Gal4 preventing transcription.

(B) During transcription activation, at the *GAL* genes nucleosomes are evicted from promoter and coding regions. Histone acetylation levels (H3-K9/H3 and H3-K14/H3) increase upon transcription induction. Upon galactose induction, Gal4 is free to activate transcription and the pre-initiation complex is recruited to the TATA box. We suspect that various chromatin remodelers (HATs, ATP-dependent remodelers, and histone chaperones) are recruited to the DNA to modify the chromatin structure.

CHAPTER 4 NAP1 CONTRIBUTIONS TO HISTONE MODIFICATIONS AT THE *GAL* LOCUS

4.1. ABSTRACT

The eukaryotic genome is organized into chromatin, containing repeating units of nucleosomes whose dynamics greatly influence chromatin architecture. The highly compact nature of chromatin creates a barrier for enzymes that require access to DNA during replication, transcription, and DNA repair. During transcription, histone chaperone-dependent histone exchange occurs at promoter and coding regions to allow efficient synthesis of mRNA. Here, we analyze the contribution of Nap1 to guided nucleosome assembly and histone acetylation at galactose inducible genes *in vivo*. Our approach is highly sensitive and allows comparison of histone occupancy and acetylation status of histones upon gene activation. We show that the histone chaperone Nap1 in addition to its role in histone assembly, may also function in nucleosome disassembly. We propose a plausible model of the mechanism of action of yeast Nap1 role in chromatin dynamics at galactose inducible genes.

4.2. INTRODUCTION

The organization of eukaryotic DNA into chromatin influences many DNA-associated processes, including transcriptional regulation. Each repeating unit, the nucleosome, displays important chemical and structural information that dictates chromatin architecture. For example, nucleosomes are disassembled from many eukaryotic promoters during transcriptional activation to provide access to the general transcription machinery ⁴⁰. Thus, the way in which nucleosomes are exchanged on DNA can impact not only the stability of chromatin structure, but also patterns of gene expression. Histone chaperones are acidic proteins that bind and exchange specific histones, thereby preventing incorrect histone-DNA interactions. Additionally, histone chaperones can temporarily remove histones from DNA to allow the passage of RNA polymerase during gene transcription ⁴¹. Histone acetyltransferases (HAT) are proteins that

catalyze the acetylation of histones, which results in important regulatory effects on chromatin structure and gene transcription. Here, we determine the effects of the deletion *NAP1* on histone H3 occupancy and acetylation status at galactose inducible genes. The *GAL* genes bear nucleosomes that occupy promoter and coding regions prior to gene activation, and histone mobilization is an important aspect of Gal4-dependent gene activation from these promoters³³.

4.3 RESULTS

NAP1 IS NECESSARY FOR NORMAL HISTONE H3 OCCUPANCY AT INACTIVE *GAL* GENES

In Chapter 3, initial histone H3 occupancy was measured at amplicons spanning the *GAL* genes during growth in repressive conditions (raffinose media). Next, we determine if deletion of *NAP1* altered histone H3 occupancy at inactive *GAL* genes (See equation 1 for histone H3 normalized occupancy calculation in Materials and Methods Chapter). Using chromatin immunoprecipitation assays, we observed a significant decrease in histone H3 levels at promoter and coding regions of the *GAL* genes during repressive conditions in cells depleted of Nap1 (Fig. 4.1). To test if this effect is global, H3 levels were assessed from whole cell extracts from cells depleted of Nap1. It was observed that global H3 levels are comparable to wild-type in repressive and activating conditions (Supplemental Fig.1). This evidence suggests that the decreased levels of histone H3 in the *NAP1* deletion strain are specific to the *GAL* genes. Next, we observed histone H3 occupancy during activating conditions (growth in galactose). We observed that histone H3 levels at *GAL* genes are comparable to wild-type in cells lacking Nap1 (Fig. 4.2).

NAP1 IS NECESSARY FOR NORMAL HISTONE H3 EVICTION UPON TRANSCRIPTION ACTIVATION

As previously described (Chapter 3), nucleosomes are evicted from promoter and coding regions when cells are grown in galactose. Next, we determined the effect of *NAP1* deletion on histone H3 eviction profiles upon galactose induction

(Fig. 4.3). We plotted cells lacking Nap1 eviction profiles against wild-type eviction profiles (Fig. 4.4). Cells lacking Nap1 were unable to evict during the first 10 minutes of galactose induction. Interestingly, after 20 minutes of growth in galactose, histone H3 occupancy in Nap1 depleted cells similar to wild-type histone H3 occupancy. However, after 60 minutes of growth in galactose histone H3 occupancy in the *NAP1* deletion strain does not reach that of wild-type levels. Interestingly, deletion of *NAP1* did not significantly affect the histone H3 eviction profiles of two *GAL* amplicons. We showed that the *GAL7* UAS (Chapter 3) did not evict to the same extent as the other amplicons from 0-10 minutes of growth in galactose. We observed the same result in cells lacking Nap1. Additionally, the H3 eviction profile between wild-type cells and cells lacking Nap1 looked identical at the *GAL7* UAS throughout the rest of the galactose time course. The *GAL10* 5' ORF is another amplicon whose H3 eviction profile was not altered upon *NAP1* deletion. This region was the only amplicon where H3 evicted during 0-10 minutes of galactose induction when Nap1 was depleted. Thus, Nap1 does not appear to have a role in histone H3 eviction at the *GAL7* UAS and *GAL10* 5' ORF. However, the earlier eviction kinetics of histone H3 at the rest of the *GAL* locus was severely altered upon *NAP1* deletion.

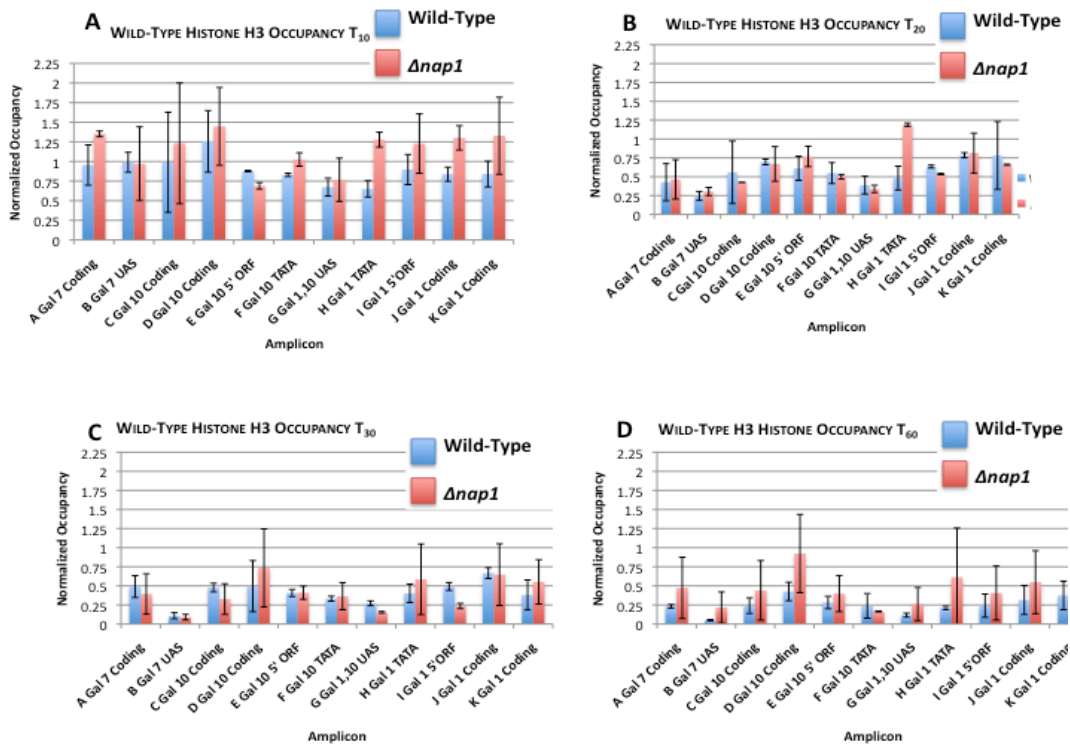


FIGURE 4.2 CELLS LACKING NAP1 CONTAIN SIMILAR LEVELS OF HISTONE H3 OCCUPANCY DURING ACTIVATING CONDITIONS

ChIP analyses of histone H3 occupancy at galactose inducible promoters and coding regions were performed after growth in galactose media for wild-type and $\Delta nap1$ cells during (A) 10 minutes T_{10} (B) 20 minutes T_{20} (C) 30 minutes T_{30} (D) 60 minutes T_{60} of growth in galactose media at amplicons A-K. Each study was performed in duplicate, and normalized to a telomere control. Hatch marks indicate non-linear time on the x-axis.

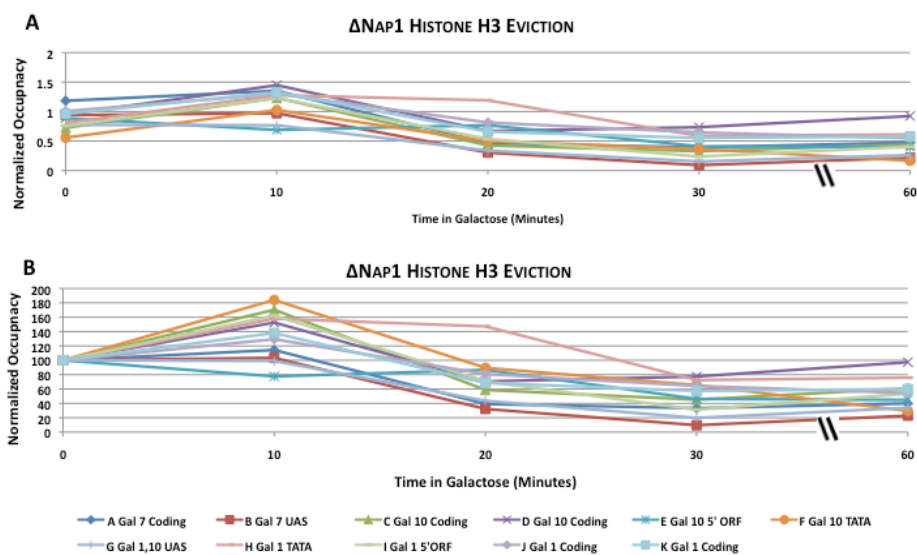


FIGURE 4.3: CELLS LACKING NAP1 DISPLAY DELAYED HISTONE H3 EVICTION UPON TRANSCRIPTION

ChIP analyses of histone H3 (anti-H3) at galactose inducible promoters and coding regions were performed in raffinose (T_0) or galactose (T_{10} T_{20} T_{30} T_{60}) in cells lacking Nap1. **(A)** Normalized histone H3 occupancy **(B)** Initial normalized histone H3 occupancy (T_0) was set to 100 and additional time points were adjusted to this value. Each study was performed in duplicate, and normalized to a telomere control. Hatch marks indicate non-linear time on the x-axis.

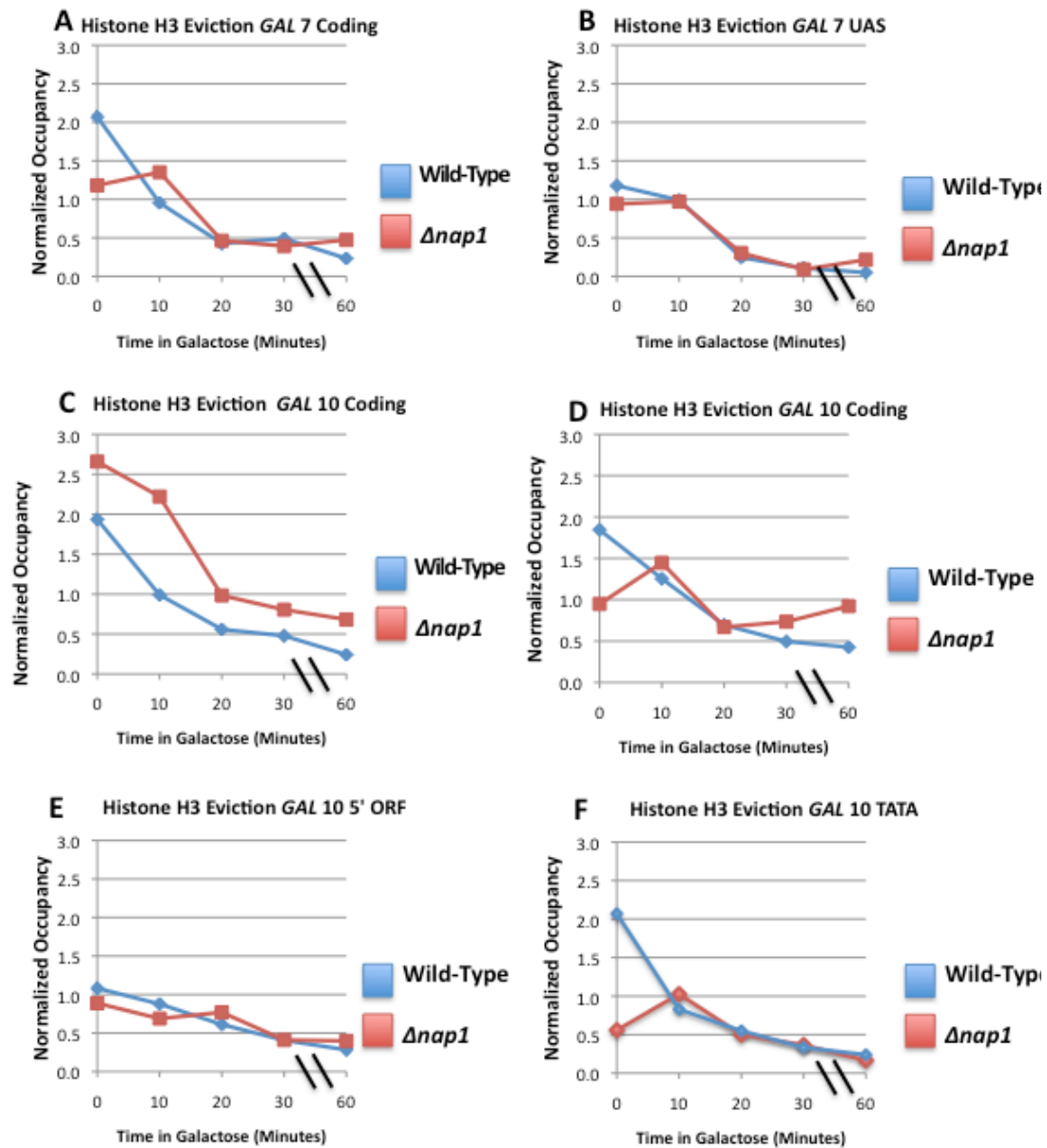
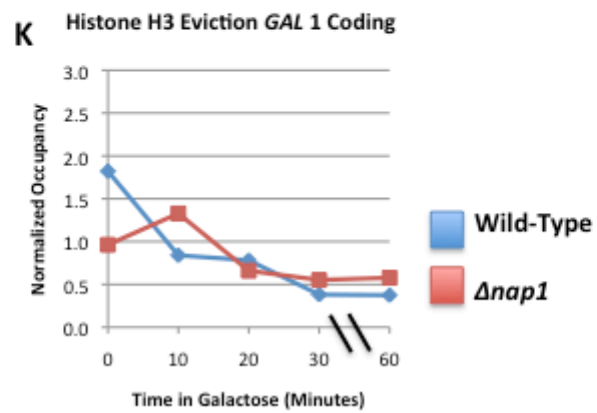
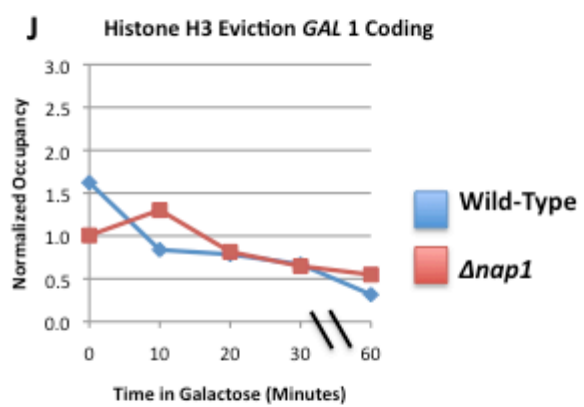
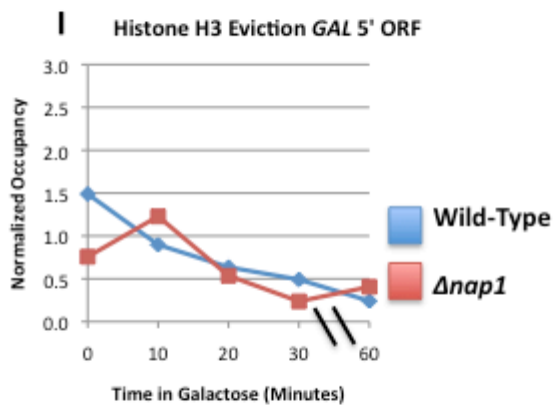
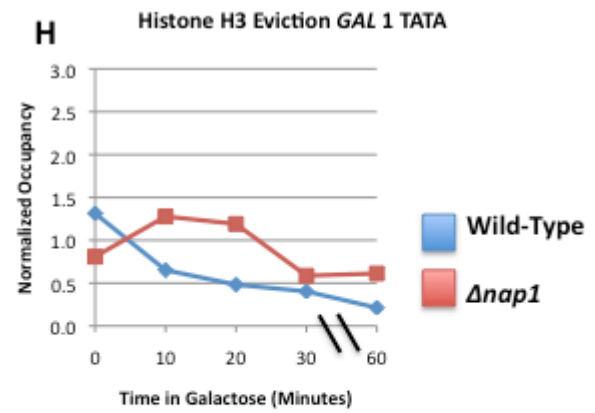
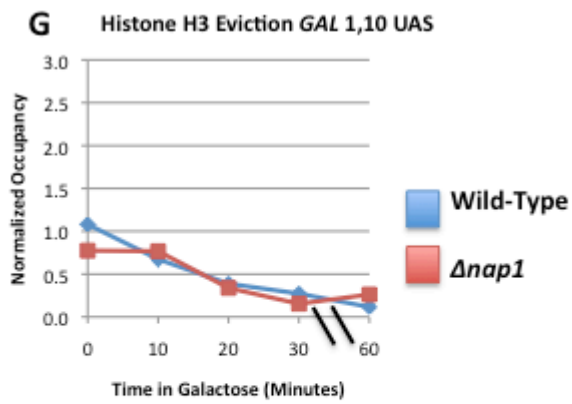


FIGURE 4.4: CELLS LACKING NAP1 DISPLAY DELAYED H3 EVICTION UPON TRANSCRIPTION ACTIVATION

ChIP analyses of histone H3 (anti-H3) at galactose inducible promoters and coding regions were performed in raffinose (T_0) or galactose (T_{10} , T_{20} , T_{30} , T_{60}) in cells lacking Nap1 at amplicons **A-K**. Each study was performed in duplicate, and normalized to a telomere control. Each study was performed in duplicate, and normalized to a telomere control. Hatch marks indicate non-linear time on the x-axis.



CELLS LACKING Nap1 HAVE DECREASED ABSOLUTE HISTONE H3 EVICTION RATES AT GAL GENES

In the previous chapter, we determined the eviction rate of histone H3 at each ChIP amplicon (A-K). The absolute histone H3 eviction rate (Initial Occupancy-Lowest Occupancy / Time, Equation 5 in Materials and Methods Chapter) range observed was between 1.33-4.73 acetylation units/minute. Next, we wanted to know if deletion of *NAP1* affected the kinetics of histone H3 eviction. We observed a decrease in absolute histone H3 eviction rate at the majority of the amplicons analyzed in cells lacking Nap1 (Fig. 4.5). The absolute histone H3 eviction range observed was between 0.66-2.83 H3 units/minute. Interestingly, we see an increase in the histone H3 eviction rate in cells lacking Nap1 only at the UAS of *GAL7* and *GAL1*, 10. Next, we wanted to see if there were differences in acetylation rates at specific times throughout the galactose time course (Fig 4.6). During the initial 10 minutes of galactose induction (See Equation 7 in Materials and Methods Chapter), we observed a decrease in H3 eviction across the *GAL* genes in cells lacking Nap1. Rate of histone H3 eviction was not determined between 10-20 minutes of galactose induction because histone H3 failed to evict in cells lacking Nap1. Similar to initial H3 eviction, we see a decrease in the H3 eviction rate during 20-30 minutes of galactose induction (See Equation 8 Materials and Methods). During 30-60 minutes of galactose induction, we saw varying effects of NAP1 deletion on histone H3 eviction at different amplicons. The majority of amplicons showed similar H3 eviction rates (*GAL7* ORF, *GAL10* ORFs, *GAL1*, 10 UAS, and *GAL1* ORF. The *GAL10* TATA had a decreased histone H3 eviction rate while other amplicons such as the *GAL1* TATA showed increased H3 eviction rate in cells lacking Nap1.

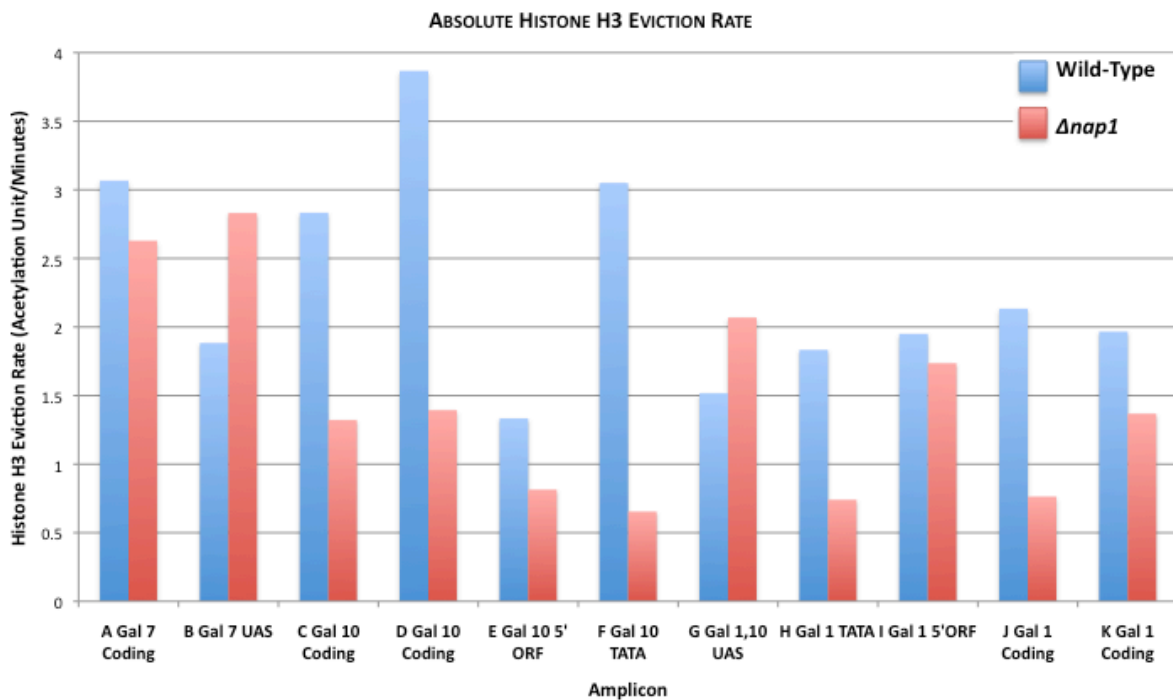


FIGURE 4.5: CELLS LACKING NAP1 HAVE DECREASED HISTONE H3 EVICTION RATES AT GAL GENES

Eviction rate was determined by subtracting the minimum histone H3 occupancy from the initial H3 occupancy (T_0) and divided by the time it took for the minimum H3 occupancy to occur during the galactose time course. Eviction rate values were determine from normalized ChIP values.

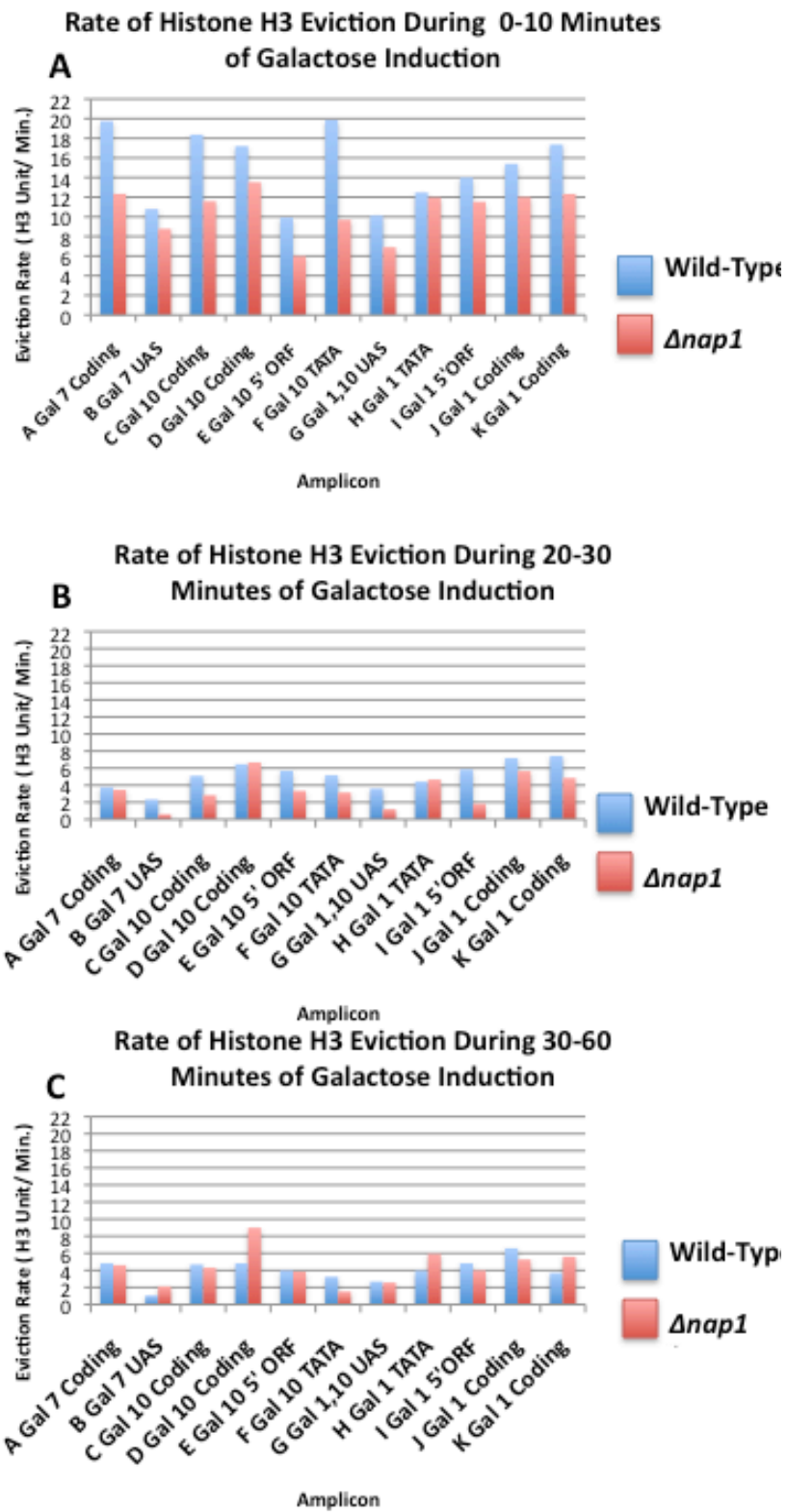


FIGURE 4.6: CELLS LACKING NAP1 HAVE DECREASED H3 EVICTION RATES AT GAL GENES
 Histone H3 Eviction rates were calculated between (A) 0-10 minutes, (B) 10-20 minutes, (C) 20-30 minutes and (D) 30-60 minutes using normalized ChIP acetylation values.

LOW LEVELS OF H3 FOUND IN CELLS LACKING NAP1 ARE HYPER-ACETYLATED AT INACTIVE *GAL* GENES

To investigate the *in vivo* relationship between histone acetyltransferases and histone chaperones at the *GAL* locus; we determined the consequence of loss of Nap1 function on histone H3-K9/H3 and H3-K14/H3 acetylation (See Equation 6 in Materials and Methods for histone H3 normalization calculation). In Chapter 3, we determined the amount of acetylation (H3-K9/H3 and H3-K14/H3) that was present in wild-type cells during repressive conditions. Using ChIP analysis, we see that the low amounts of H3 present in the *NAP1* deletion strain at the promoter and coding regions are hyper-acetylated at H3-K9/H3 at inactive *GAL* genes (Fig. 4.7). However, we do not observe an increase in H3-K14/H3 acetylation at the *GAL* genes.

CELLS LACKING NAP1 HAVE SIMILAR LEVELS OF ACETYLATION AS WILD-TYPE CELLS AT ACTIVE *GAL* GENES

Nap1 is needed for normal histone K9-H3 acetylation levels at inactive *GAL* genes. Next, we wanted to determine if Nap1 had an effect on acetylation level at active *GAL* genes (Fig 4.8). We observed that when cells were grown in galactose media, cells lacking Nap1 contained similar levels of H3-K9/H3 acetylation as wild-type cells. However, we did see some amplicons that contained higher levels of H3-K14/H3 at active *GAL* genes. It appears that even though Nap1 has an effect on the density of acetylation during repressive conditions, it does not play as big of a role of kinetics of acetylation during activating conditions.

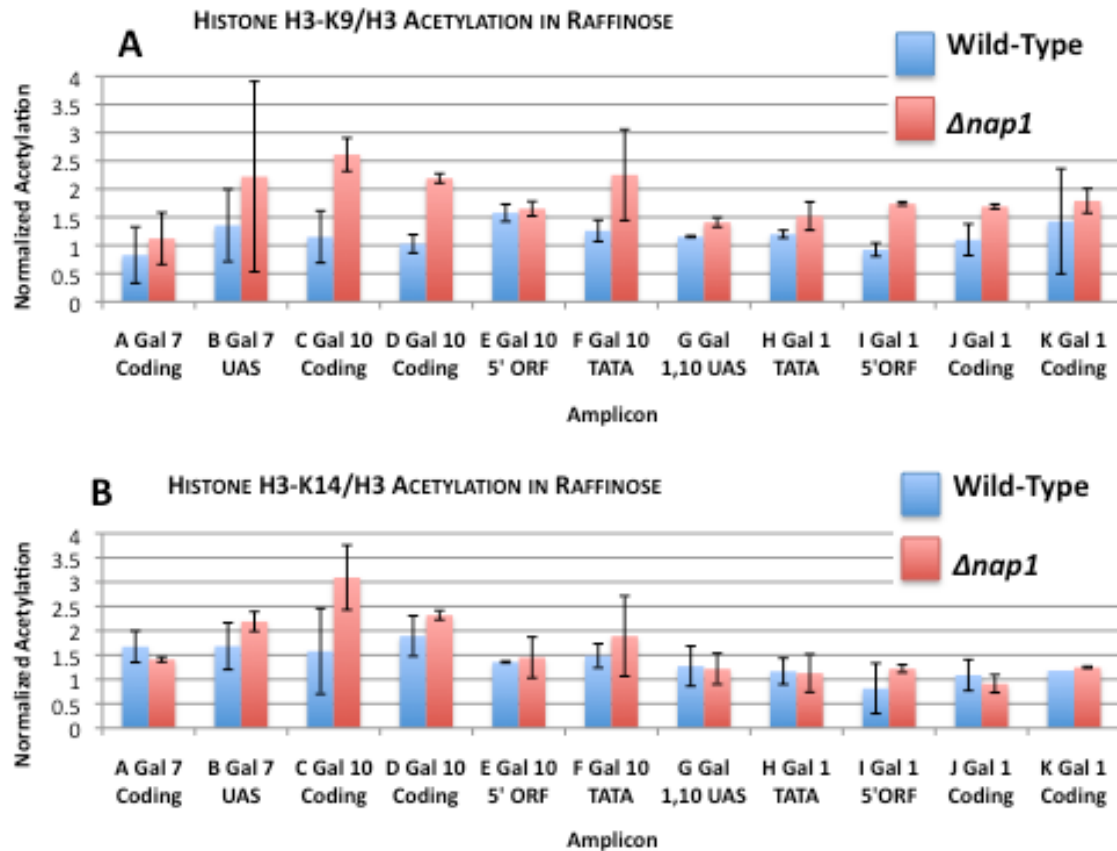


Figure 4.7: CELLS LACKING NAP1 HAVE INCREASED H3-K9 ACETYLATION IN REPRESSIVE CONDITIONS

ChIP analyses of (A) acetylated histone H3-K9/H3 and (B) histone H3-K14/H3 were performed on wild-type or $\Delta nap1$ cells grown in raffinose. Each column corresponds to the location of a real-time PCR amplicon. Error bars indicate standard deviations from two independent biological replicates and values were normalized to a telomere control.

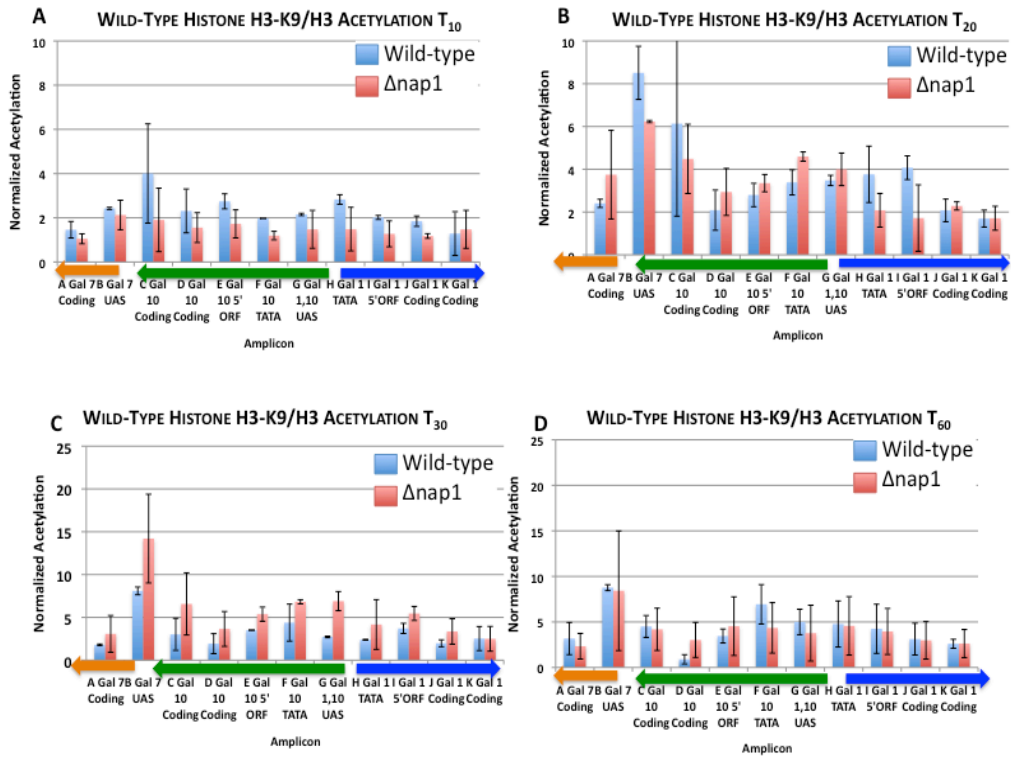


Figure 4.8: CELLS DEPLETED OF Nap1 CONTAIN SIMILAR LEVELS OF ACETYLATION AT ACTIVE GAL GENES

ChIP analyses of histone H3-K9 (A-D) at galactose inducible promoters and coding regions were performed in galactose (T₁₀T₂₀T₃₀T₆₀) in cells lacking Nap1 at amplicons A-K. Each study was performed in duplicate, and normalized to a telomere control. Error bars indicate standard deviations from two independent biological replicates and values were normalized to a telomere control.

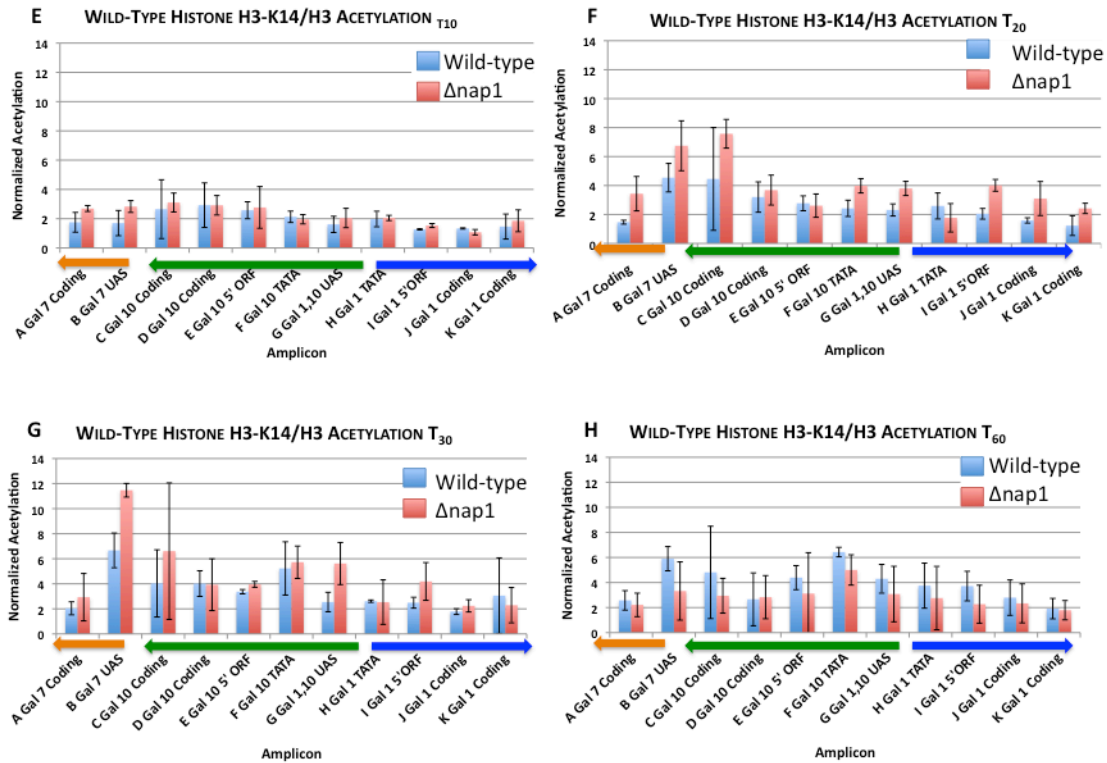


FIGURE 4.8: CELLS DEPLETED OF NAP1 CONTAIN SIMILAR LEVELS OF ACETYLATION AT ACTIVE GAL GENES

ChIP analyses of histone H3-K14 (E-H) at galactose inducible promoters and coding regions were performed in galactose (T₁₀ T₂₀ T₃₀ T₆₀) in cells lacking Nap1. Each study was performed in duplicate, and normalized to a telomere control. Error bars indicate standard deviations from two independent biological replicates and values were normalized to a telomere control.

NAP1 IS NECESSARY FOR NORMAL ACETYLATION KINETICS

Histone H3 acetylation ChIP values were used to calculate the time at which half maximum acetylation (H3-K9/H3 and H3-K14/H3) occurred (See Materials and Methods for method of determining the time of half maximum histone H3 acetylation. The highest amount of acetylation observed during galactose media was set to 100 and other time values were normalized to this value. A plot was constructed of normalized acetylation versus time in galactose. The amount of half acetylation was determined by subtracting the starting amount of acetylation from the maximum acetylation observed divided in half. This value was added to the starting amount of acetylation to determine the amount of half acetylation specific to that amplicon. The time at which half acetylation occurred was determined by line extrapolation from the half-acetylation value. We observed that at the majority of the amplicons cells lacking Nap1 were unable to reach half maximum acetylation of K9/H3 as fast as wild-type cells (Fig. 4.9). Interestingly, cells lacking Nap1 were able to reach maximum acetylation of H3-K14/H3 faster than wild-type cells evident from an increased time at half maximum acetylation occurred.

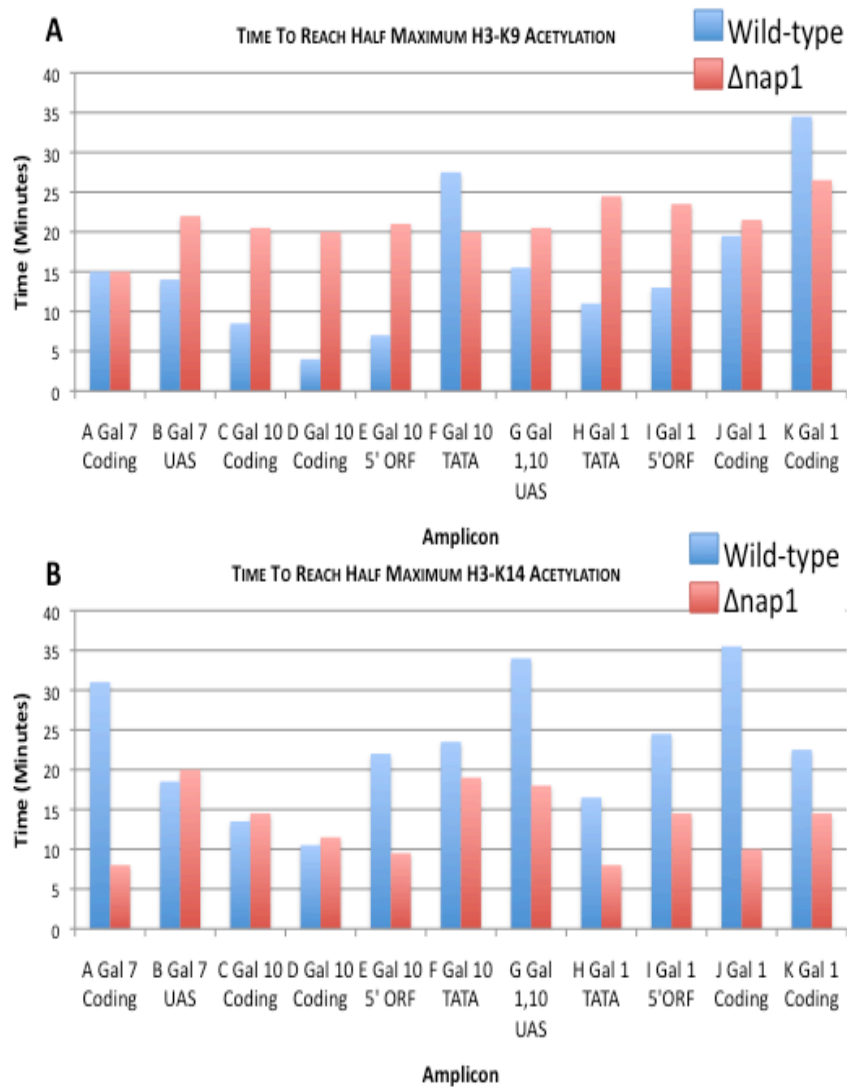


FIGURE 4.9: DELETION OF *NAP1* HAS A DIFFERENTIAL IMPACT ON THE KINETICS OF HALF MAXIMUM HISTONE OF HISTONE H3-K9 AND H3-14 ACETYLATION AT GAL GENES

An explanation of how the time at which half maximum histone H3 acetylation occurs was determined is described in the materials and methods chapter. Time to reach half maximum histone H3 acetylation of **(A)** H3-K9 and **(B)** H3-K14 in minutes was plotted for amplicons A-K.

4.4 DISCUSSION

NAP1 IS NECESSARY FOR NORMAL HISTONE H3 OCCUPANCY AT INACTIVE *GAL* GENES

We observed decreased levels of histone H3 at the *GAL* locus during growth in raffinose in cells lacking Nap1. This creates an abnormal chromatin environment even before transcription is initiated. Nap1 is necessary to inhibit non-productive nucleosome interactions by preventing the littering of H2A/H2B dimers on the DNA⁴. Our proposed model is that Nap1 is needed to remove the littering of H2A/H2B dimers and aid in the assembly of nucleosomes at the *GAL* genes. Upon transcription activation, cells lacking Nap1 failed to evict nucleosomes during the initial 10 minutes of galactose induction. It is thought that nucleosomes are displaced from promoter regions by chromatin-remodeling complexes. The nucleosome remodeling complex SWI/SNF removes promoter nucleosomes in an early step in the process of gene induction⁴². It is plausible that in the absence of Nap1, SWI/SNF is unable to be recruited to the chromatin to evict nucleosomes. Here, our model presents Nap1's role of nucleosome assembly during transcription repression (Fig.4.10) and histone eviction (Fig.4.11) during transcription activation. At inactive *GAL* genes, nucleosome density was decreased in the absence of Nap1. When Nap1 is present it is responsible for assembling the H2A-H2B dimers on the H3-H4 tetramer to form the nucleosome. At active *GAL* genes, histone H3 is not evicted from promoter and coding regions in the absence of Nap1. We hypothesize that Nap1 is necessary for the recruitment or function of ATP-dependent chromatin remodelers. Alternatively, it is possible that Nap1 is independently responsible for initial histone H3 eviction at *GAL* genes. Cells lacking Nap1 contain lower levels of histone H3, which contain increased acetylation on histone H3-K9 at inactive *GAL* genes. These results are historically correlated with active genes. The chromatin environment in cells lacking Nap1 during repressive conditions seems to already be "open to transcription". Upon transcription activation, we see that histone H3 does not evict during the first 10 minutes of growth in galactose. However, this lack of eviction does not appear to hamper transcription as cells lacking Nap1 have

increased transcription kinetics at the *GAL* genes ⁴. Additionally, we see that Nap1 also plays a necessary role in H3 eviction after 20 and 30 minutes in galactose. Cells lacking Nap1 never reach the H3 eviction levels of wild-type cells. Here we present a model of how Nap1 could function at inactive *GAL* genes to prevent increased acetylation of histone H3-K9. Furthermore, we show how Nap1 functions at active *GAL* genes to insure proper H3 eviction. There are two possible mechanisms that explain how Nap1 prevents histone H3-K9 hyper-acetylation during transcription repression. Nap1 could sequester the HAT and prevent it from hyper-acetylating H3-K9. Alternatively, Nap1 could be responsible for removing the hyper-acetylated nucleosomes from the chromatin during repressive conditions. Thus, determining which mechanism is the correct one, and which HAT is responsible for the increased histone H3-K9 acetylation found at the *GAL* genes in the absence of Nap1 is of great interest.

INACTIVE GAL GENES

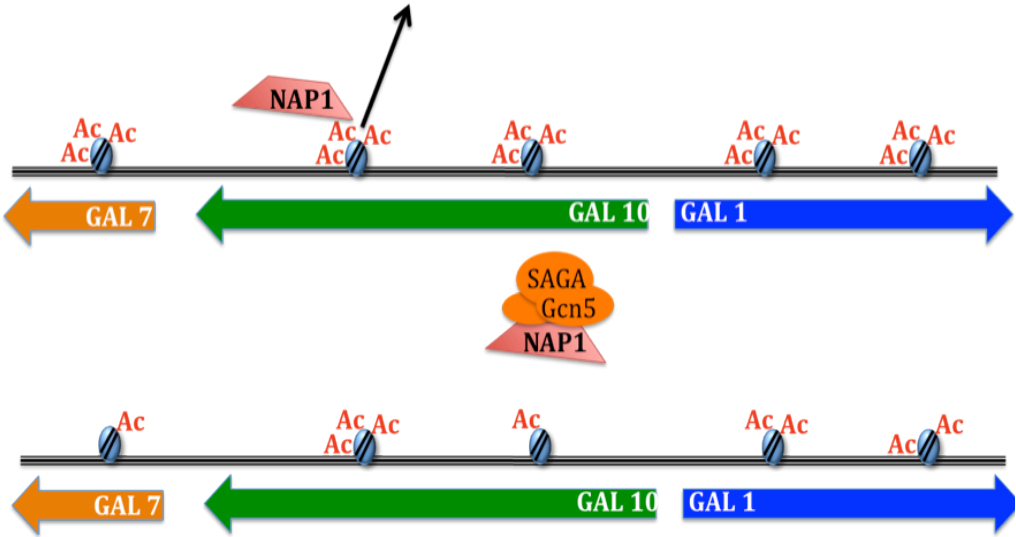


FIGURE 4.10: NAP1 IS NECESSARY FOR PREVENTING INCREASED ACETYLATION AT INACTIVE GAL GENES

At inactive GAL genes, Nap1 functions to prevent hyper-acetylation of histone H3-K9. NAP1 could be responsible for disassembling nucleosomes that are hyper-acetylated. (B) Alternatively, Nap1 could be responsible for preventing HATs from over acetylating histone H3-K9.

INACTIVE GAL GENES

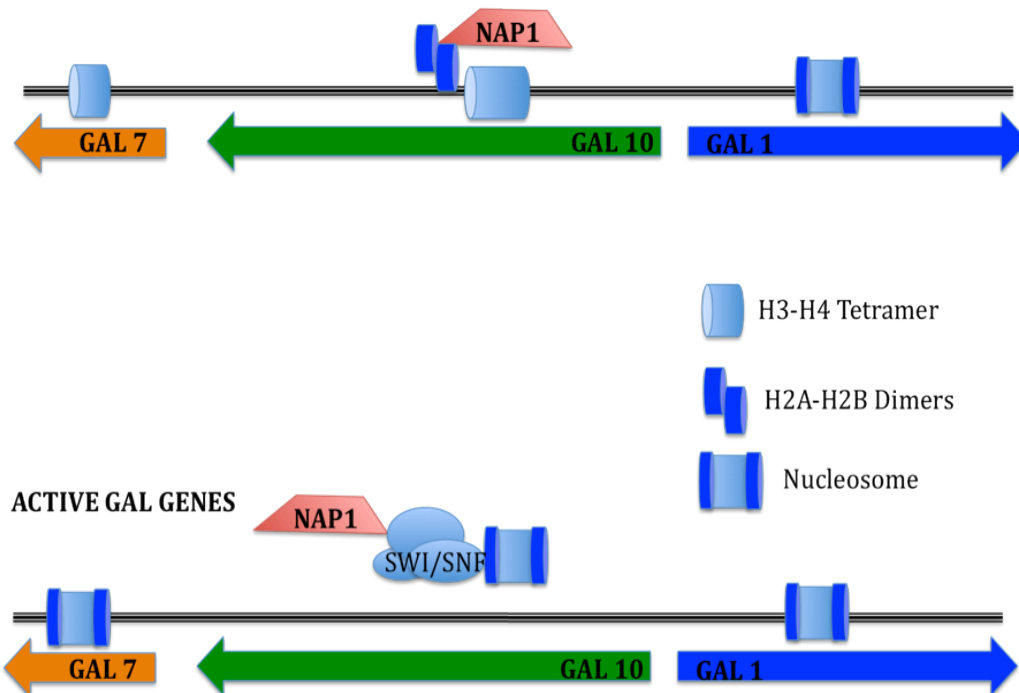


FIGURE 4.11: Nap1 ASSEMBLES NUCLEOSOMES AT INACTIVE *GAL* GENES AND PLAYS A ROLE IN NUCLEOSOME EVICTION AT ACTIVE GENES

(A) During transcription repression, Nap1 is responsible for the assembly of nucleosomes at *GAL* promoter and coding regions.

(B) During transcription activation, Nap1 is needed for the recruitment/function of chromatin remodelers for the initial eviction of nucleosomes at *GAL* promoter and coding regions.

CHAPTER 5 ASF1 AND VPS75 CONTRIBUTIONS TO HISTONE EVICTION AND MODIFICATIONS AT GALACTOSE INDUCIBLE PROMOTERS

5.1 ABSTRACT

Histone eviction from promoter regions is a potential mechanism for transcriptional regulation in eukaryotes. We investigated whether the yeast histone chaperones, Asf1 and Vps75, mediate histone H3 eviction from the UAS and TATA box of the yeast *GAL* genes upon transcriptional activation. Additionally, histone acetylation is often associated with gene activation. Here, we explore the contribution of Asf1 and Vps75 on acetylation of histones H3 tails at galactose inducible genes.

5.2. INTRODUCTION

Eukaryotic DNA is organized into chromatin that contains repeating units of nucleosomes each consisting of two histone H2A-H2B dimers and one histone H3-H4 tetramer around which 147 base pairs of DNA are wrapped. The packaging of the DNA by nucleosomes appears to affect all stages of transcription including pre-initiation complex (PIC) formation and elongation⁴³. Nucleosomes are repressive to transcription initiation and found at most gene promoters. There exist several important methods for relieving this inhibition, including post-translational modifications of histones, incorporation of histone variants, and the action of chromatin remodelers⁴⁴. Histone chaperones are required for nucleosome displacement at specific promoters^{16; 45; 46} and to a lesser extent within coding regions when a gene is activated⁴⁷. It is clear from ChIP studies that histones are lost at the yeast *PHO5* and *HSP82* promoters upon gene activation and that nucleosomes are reassembled as a gene turns off^{29; 30; 48; 49; 50}. Typically, histone acetylation occurs at multiple lysine residues and

is usually carried out by a variety of histone acetyltransferase complexes⁵¹. This study examines the role of the H3/H4 histone chaperones in chromatin dynamics to determine the changes that occur in chromatin during transcription. Histone chaperones are proteins that bind histones and mediate chromatin dynamics⁵². Asf1 is a histone chaperone that plays a role in the assembly and disassembly of chromatin associated with silenced genes such as telomeric loci. Asf1 is a highly conserved histone chaperone that binds and transfers the H3-H4 histone dimer^{52; 53; 54}. Asf1 is required for H3 eviction during transcription elongation, and Asf1 binds to promoters and coding regions of active genes¹⁸. Nucleosome disassembly is mediated by Asf1 at the *PHO5* promoter¹⁶, and exchange of histone H3 at promoters^{55; 56}. Vps75 is part of the NAP domain family of histone chaperones and can assemble nucleosomes *in vitro*¹². Additionally, Vps75 acts as a potent stimulator of the histone acetyltransferase Rtt109 and is associated with higher levels of histone H3 lysine 9 (H3-K9) acetylation^{25; 57}. Furthermore, Vps75 localizes primarily to sites of active transcription and interacts with RNAPII and other factors involved in transcription and chromatin function. Although histone eviction is necessary for efficient transcription initiation, factors that mediate such eviction *in vivo* have not been identified.

5.3 RESULTS

VPS75 IS NECESSARY FOR NORMAL HISTONE OCCUPANCY AT INACTIVE *GAL* GENES

In Chapter 3, we determined the amount of histone H3 occupancy found at *GAL* promoter regions during growth in raffinose. We wanted to see if deletions of histone chaperones, Asf1 and Vps75, would alter H3 occupancy at inactive *GAL* promoters. See Materials and Methods Equation 1 for Histone H3 normalization calculation). We see that Asf1 has similar levels of histone H3 occupancy as wild-type cells at the *GAL 1,10 UAS* and *GAL 10 TATA*. However, strains lacking Vps75 contained a 2-fold decreased in histone H3 density at the inactive *GAL 10 TATA* box and *GAL1, 10 UAS* in comparison to wild-type strains (Fig. 5.1). Interestingly, we observed decreased levels of histone H3 occupancy at the *GAL1, 10 UAS* when compared to the *GAL10 TATA* box.

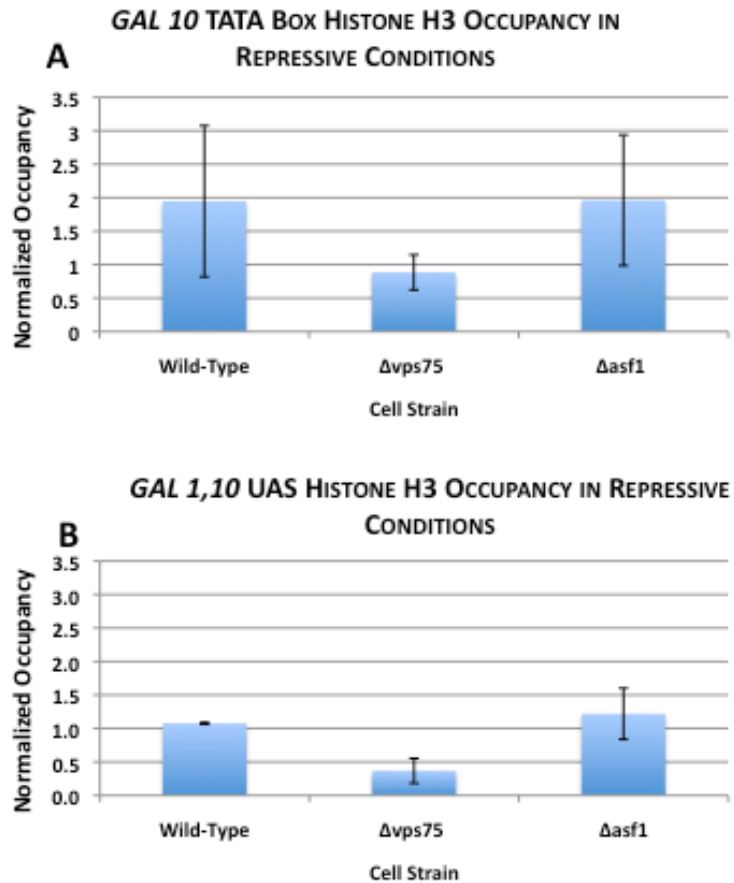


FIGURE 5.1: CELLS LACKING Vps75 EXHIBIT DECREASED LEVELS OF HISTONE H3 OCCUPANCY AT GAL LOCUS DURING REPRESSIVE CONDITIONS

ChIP analyses of histone H3 occupancy were performed on Wild-Type, $\Delta vps75$, or $\Delta asf1$ cells grown in repressive conditions (raffinose media) at (A) the GAL10 TATA Box and the (B) GAL1, 10 UAS. Error bars indicate standard deviations from two independent biological replicates.

HISTONE H3 DOES NOT EVICT UPON GALACTOSE INDUCTION IN CELLS LACKING VPS75 AT TATA BOX AND UAS

To determine histone H3 eviction profiles at the *GAL* promoter, we determined H3 occupancy at 0, 30, and 60 minutes after induction with galactose medium in wild-type cells, $\Delta asf1$, and $\Delta vps75$ strains. We observed histone H3 eviction in wild-type cells at the *GAL1*, *10* and *GAL10* UAS upon galactose induction (Fig. 5.2). Additionally, we see the same histone H3 eviction at both test amplicons in cells lacking *Asf1* (Supplemental Table 4 and 5). However, histone H3 is not evicted during the first 30 minutes of galactose induction in cells lacking *Vps75* at both the UAS and TATA box. However, after 60 minutes of growth in galactose cells depleted of *Vps75* are able to evict to similar levels of that of wild-type cells.

VPS75 IS NECESSARY TO PREVENT HYPER-ACETYLATION AT INACTIVE *GAL 1,10* PROMOTERS

Next, we explored the effect of histone chaperones deletions, $\Delta asf1$ and $\Delta vps75$, on histone acetylation at the *GAL10* promoter (TATA box and UAS) (See Equation 6 for histone H3 acetylation normalization calculation). During repressive conditions, we observed that cells lacking *Vps75* contained significant levels of increased histone acetylation of histone H3-K9 and H3-K14 at both the TATA box and UAS (Fig. 5.3). Cells lacking *Asf1* contained histone H3 acetylation levels (K9-H3 and K14-H3) that were comparable to wild-type cells.

CELLS LACKING VPS75 HAVE DECREASED HISTONE ACETYLATION RATES

Histone acetylation rates (K9/H3 and K14/H3) were determined by subtracting the initial acetylation level from the maximum acetylation level observed and divided by the time it took to reach maximum acetylation (See equation 7 in Materials and Methods Chapters for calculation). In chapter 3, we determined acetylation rates for H3-K14 and H3-K9 at the *GAL* UAS and *GAL* TATA. Next, we determined if acetylation rate was altered upon histone chaperone deletion (Fig. 5.4 and Supplemental Table 10 and 11). We observed that deletion of *ASF1* had no effect on acetylation rate of histones H3-K14/H3 and H3-K9/H3 at the *GAL10* TATA box. However, the acetylation rate of H3-K14/H3 and H3-K9/H3

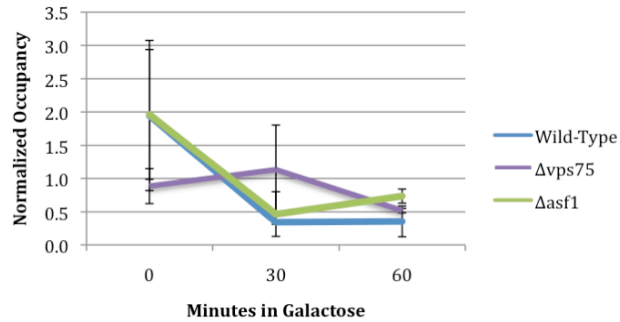
was significantly decreased in cells lacking Vps75 at the TATA box. At the *GAL1,10* UAS we see slightly decreased levels of H3-K9/H3 acetylation when compared to the *GAL10* TATA box. Deletions of histone chaperones, Asf1 and Vps75, caused a decrease in the acetylation rate of H3-K9/H3 at the *GAL1, 10* UAS. K14/H3 acetylation rate at the *GAL1, 10* UAS was not analyzed because the highest amount of acetylation in cells lacking Vps75 was in repressive conditions.

5.4 Discussion

In the *ASF1* deletion strain, H3 occupancy during repressive conditions is comparable to the wild-type strain at the *GAL1, 10* UAS and *GAL10* TATA. Deletion of *ASF1* also had little effect upon the H3-K9/H3 acetylation rates as compared to the wild-type. Interestingly, the *VPS75* deletion strain showed a marked decrease in initial (repressive conditions) H3 occupancy at the *GAL1, 10* UAS and *GAL10* TATA as well as decreased histone eviction rates during activating conditions. Also, $\Delta vps75$ strains showed aberrant histone H3-K9/14 acetylation at the TATA and UAS during repressive conditions, but decreased acetylation rates at these same residues during activating conditions.

Taken together, this data suggest that Vps75 plays a role in maintaining proper nucleosome density during repressive and activating conditions. Vps75 may also be important for preventing increased acetylation of histone H3-K9/H3, presumably by sequestering the HAT responsible for acetylating these residues. The decreased acetylation rates in activating conditions may be due to the fact that the nucleosomes were already hyper-acetylated in raffinose. Asf1 appeared to play a much smaller role in maintaining nucleosomal density and histone H3-K9/H3 acetylation rates at the *GAL1, 10* UAS and *GAL10* TATA. While deletion of this histone chaperone had little effect at these loci, it may play a larger part in regulating other genes.

A GAL 10 TATA BOX HISTONE H3 EVICTION



B GAL 1,10 UAS HISTONE H3 EVICTION

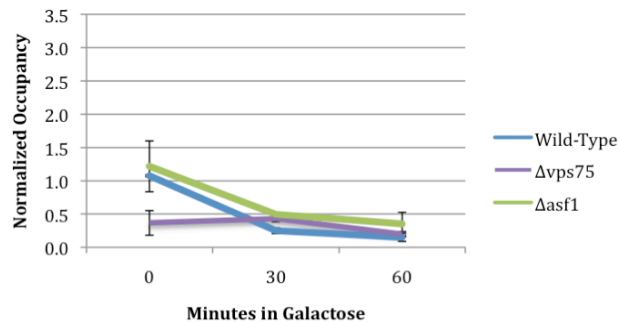
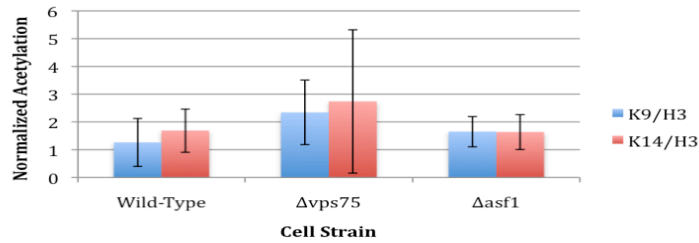


FIGURE 5.2: HISTONE H3 DOES NOT EVICT UPON GALACTOSE INDUCTION IN CELLS LACKING VPS75 AT TATA BOX AND UAS

(A) ChIP analyses of histone H3 occupancy were performed on wild-type, $\Delta asf1$, or $\Delta vps75$ cells conditions at (A) the *GAL10* TATA Box and the (B) *GAL 1,10* UAS. . Error bars indicate standard deviations from two independent biological replicates.

A GAL 10 TATA BOX HISTONE H3 ACETYLATION IN RAFFINOSE



B GAL 1,10 UAS HISTONE H3 ACETYLATION IN RAFFINOSE

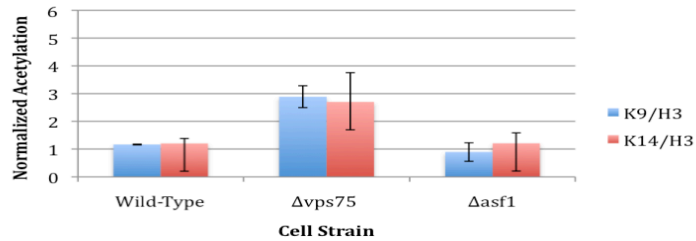


FIGURE 5.3: CELLS LACKING VPS75 CONTAIN DECREASED LEVELS OF HISTONE H3 OCCUPANCY DURING REPRESSIVE CONDITIONS

ChIP analyses of histone H3 acetylation (H3-K9/H3 and H3-K14/H3) were performed on wild-type, $\Delta vps75$, or $\Delta asf1$ cells grown in repressive conditions at (A) the *GAL10* TATA Box and the (B) *GAL1, 10* UAS. Error bars indicate standard deviations from two independent biological replicates.

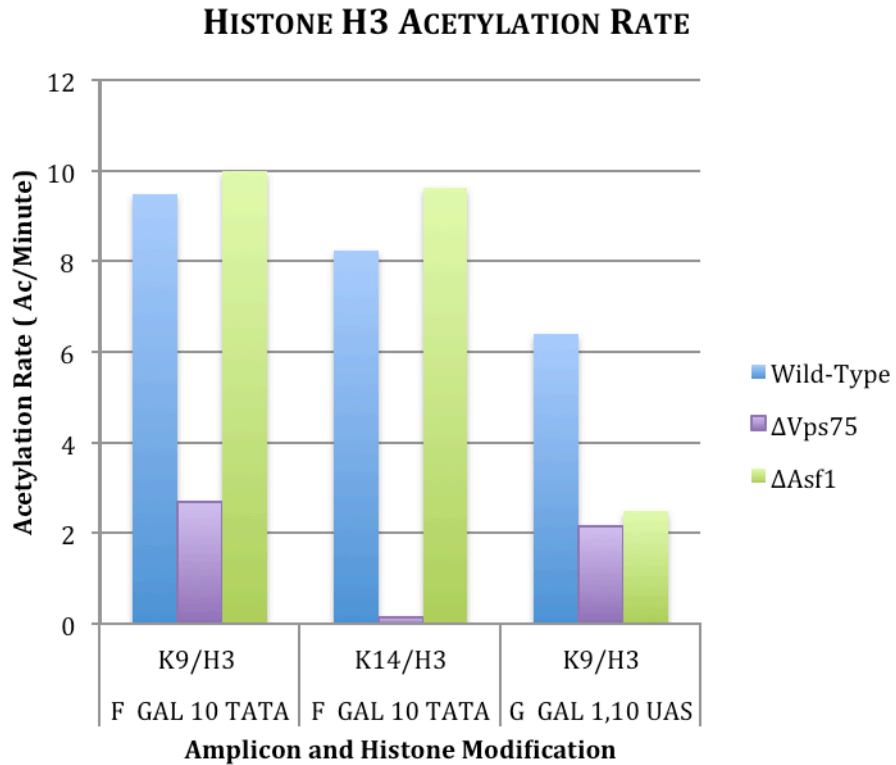


FIGURE 5.4: DELETION OF VPS75 RESULTS IN DECREASED HISTONE ACETYLATION RATES

Acetylation rate was determined by subtracting initial normalized acetylation values (T_0) from the maximum normalized acetylation value and divided by the time it took for this maximum acetylation to occur during the galactose time course.

CHAPTER 6 CHARACTERIZATION OF HISTONE CHAPERONE-GFP FUSION PROTEINS

6.1 ABSTRACT

Cells contain discrete complexes of histone chaperones, each of which may perform independent biological functions. Often the key indicator of the function of a protein is the identification of molecules with which it directly interacts. A fluorescence detection system for analytical ultracentrifuge (F-AUC) provides an innovative tool for studying macromolecular complexes in solution. Here, two methods are used to determine the fluorescent intensity and wavelength distribution of the emission spectrum of endogenously expressed GFP-histone chaperones fusion proteins. Additionally, this work gives insight into solutions to reduce auto-fluorescence found in *S. cerevisiae*. Thus, utilization of these techniques will allow for the accurate detection of GFP-histone chaperones and determination of sedimentation parameters.

6.2 INTRODUCTION

Yeast histone chaperones are necessary for normal acetylation patterns *in vivo* (Chapter 3). Thus, we expect to find interactions between histone chaperones and HATs. Indeed, Vps75 and Asf1 have been shown to co-purify with Rtt109⁵⁸;⁵⁹. Additionally, histone chaperones are needed for the exchange of H3/H4 that occurs during transcription⁵⁵. Therefore, it is likely that histones chaperones are found in large complexes with proteins such as SAGA that are required for functional interactions. F-AUC will allow for the determination of the solution state properties of endogenous histone chaperones that will ultimately give insights into the potential complexes in which histone chaperones exist.

Historically, AUC has played an important role in the characterization of protein complexes⁶⁰. We have access to one of the few analytical ultracentrifugation facilities in the world that possesses a fluorescence detection system. Fluorescence detection allows for increased sensitivity of the instrument permitting the use of decreased concentrations of sedimenting molecules

compared to that required for absorbance-detected sedimentation. Additionally, due to the remarkable selectivity of fluorescence detection, it is possible to characterize the sedimentation behavior of GFP-labeled proteins in cell lysates without further purification. We have obtained strains expressing GFP-tagged derivatives of Nap1, Vps75, and Asf1 (Invitrogen). Each histone chaperone-GFP strain contains an open reading frame with a C-terminal *Aequorea victoria* GFP (S65T) fusion tag⁶¹. The histone chaperone-GFP fusion proteins are integrated into the yeast chromosome through homologous recombination and are expressed from endogenous promoters. Most importantly, our GFP fusion proteins maintain the normal functions and localizations of the host histone chaperones³⁶. Genetically encoded fluorescent proteins are used in a variety of applications including live-cell imaging, localization of proteins, and interactions between proteins^{62; 63; 64}. To determine biophysical sedimentation properties of endogenous histone chaperones, clarified whole cell extracts of *S. cerevisiae* expressing GFP-Vps75, GFP-Nap1, or GFP-Asf1 will be subjected to fluorescence detected sedimentation velocity and sedimentation equilibrium measurements. In sedimentation velocity experiments, the movement of solutes in high centrifugal fields is used to define the size, shape and interactions of macromolecules. Alternatively, sedimentation equilibrium is a thermodynamic method where equilibrium concentration gradients at lower centrifugal speeds are analyzed to define complex molecule mass, stoichiometry, association constants and solution homogeneity. After measuring sedimentation and equilibrium parameters of histone chaperone-GFP strains, we will also characterize the properties of the chaperones in strains deleted for HATs. However, before determining sedimentation and equilibrium velocity profiles for our GFP-tagged histone chaperones, it is important to quantify the expression levels and measure the parameters of fluorescence of our fusion proteins. Here we use two techniques, fluorescence spectroscopy and fluorescence microscopy, to characterize the fluorescent intensity and wavelength distribution of emission spectrum in yeast cells expressing GFP-histone chaperon fusion proteins.

6.3 RESULTS

Western blot analysis revealed the expression levels of histone chaperone-GFP fusion proteins and verified the presence of a GFP tag (Fig. 6.1). Both Asf1-GFP and Vps75-GFP display slightly decreased levels of expression compared to that of Nap1-GFP. One logical explanation for this difference in expression levels is that the number of molecules per cell of the histone chaperones is different. Global analysis of protein expression in yeast reports the presence of 8070 molecules per cell of Nap1, 6230 molecules per cell of Asf1, and 3120 molecules per cell of Vps75, which parallel relative expression levels shown here ⁶⁵. Lastly, we observed an increase in the molecular weight of Nap1, Asf1, and, Vps75 by 27 kDa, indicating that our histone chaperones are fused to a GFP tag.

A spectrofluorometer provides one of the most straightforward techniques to measure total fluorescence from a cell population. This technique is a useful way to evaluate the GFP spectra *in vivo*, quantitative GFP signal, and most importantly aid in calibration of the F-AUC. The intensity and wavelength distribution of the emission spectrum after light excitation was measured by a Horiba Jobin Yvon Fluorolog-3 spectrofluorometer. The emission spectrum for each of the fluorescent fusion histone chaperones is shown (Fig. 6.2) Interestingly, Nap1-GFP and Asf1-GFP display an increased peak fluorescence signal when excited at 488 nm compared to that of Vps75-GFP and the untagged (wild-type) strain. The lower fluorescent signal found in Vps75-GFP fusion proteins could be due to the decreased expression levels

Additionally, fluorescence microscopy was used to visualize the presence and examine the intensity of histone chaperone-GFP proteins *in vivo* (Fig. 6.3). Nap1, Vps75, and Asf1 cells display slightly more intense fluorescence than background levels (untagged wild-type). Consistent with the results of the spectrofluorometer, wild-type cells contained a high amount of auto-fluorescence.

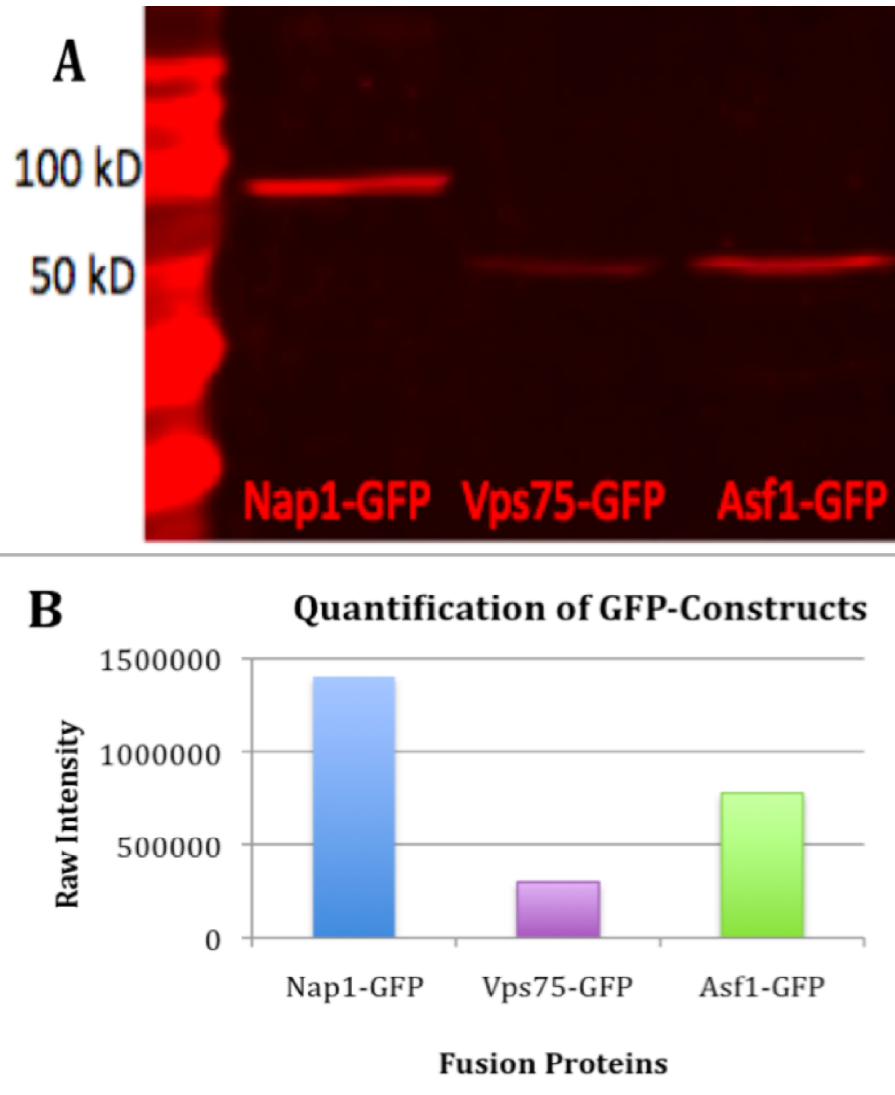


FIGURE 6.1: HISTONE CHAPERONE-GFP FUSION PROTEINS
(A) 20 μ g of whole cell extracts grown containing Nap1-GFP, Vps75-GFP, or Asf1-GFP were separated by 15% SDS gel electrophoreses, transferred to a nitrocellulose membrane, and probed with anti-GFP antibody. (B) Quantification of expression levels of GFP-histone chaperone fusion proteins.

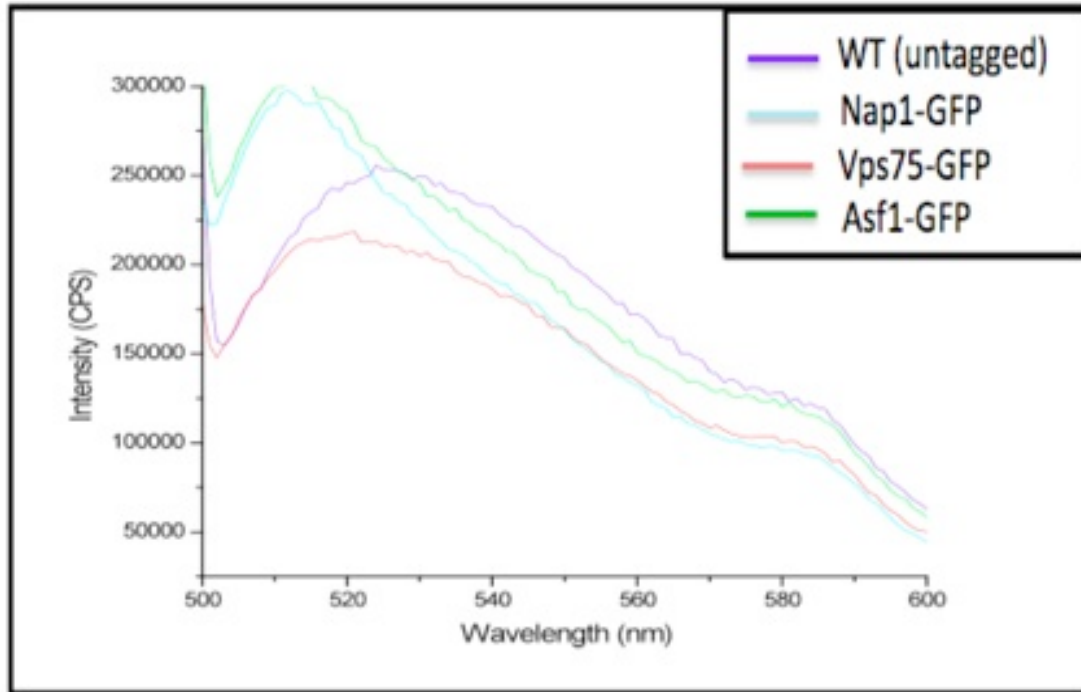


FIGURE 6.2: EMISSION SPECTRUM OF *S. cerevisiae* CELLS EXPRESSING HISTONE CHAPERONE-GFP FUSION PROTEINS
Emission spectrum of GFP-fusion proteins and the untagged wild-type (WT) was determined by excitation of light at 488 nm wavelength.

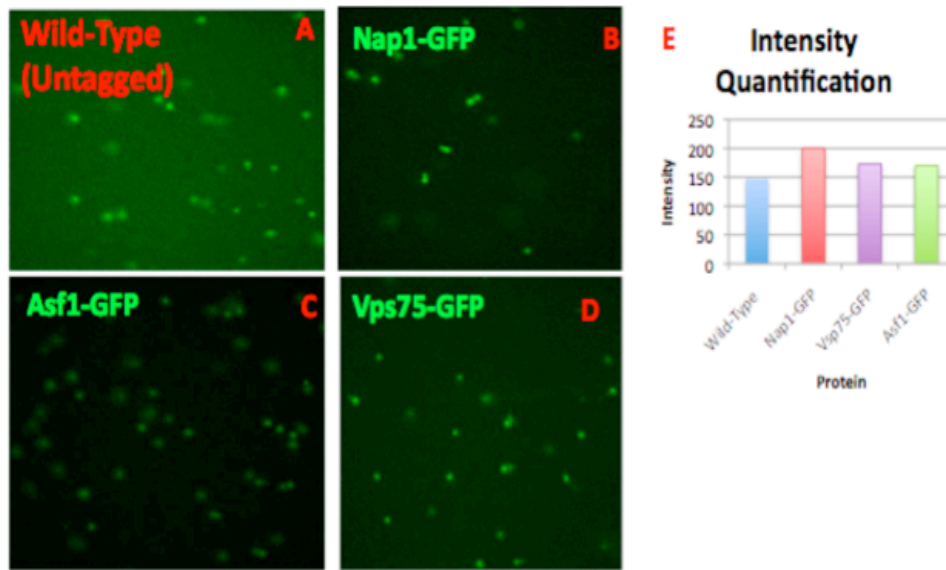


FIGURE 6.3: SACCHAROMYCES CEREVISIAE HISTONE CHAPERONE-GFP FUSION PROTEINS

Fluorescent histone chaperones (B) Nap1-GFP (C) Asf1-GFP and (D) Vps75-GFP tagged on the carboxyl terminus allows for analysis and (E) quantification of intensity when illuminated at 488 nm. (A) Wild-Type (untagged) cells used as a control.

6.5 DISCUSSION

We employed multiple techniques to measure fluorescence parameters of histone chaperone-GFP fusion proteins for the application of studying protein interactions in solution using F-AUC. After characterization of the fluorescent intensity and wavelength distribution of emission spectrum, we concluded that accurate detection of a peak fluorescence molecule would be difficult. The detectability of a fluorescent protein is a function of the brightness of the tagged protein and the auto-fluorescence within the cell.

The intrinsic brightness of a fluorescent protein (defined as the product of the fluorescent quantum yield and the extinction coefficient) is dependent on the sequence of the fusion protein and by the surrounding medium ⁶⁶. Of great importance is the absolute brightness of the fluorescent proteins relative to the background fluorescence. Hence, the brighter the endogenous auto-fluorescence, the brighter a tagged protein must be in order to be detected above background. There are naturally occurring fluorescent metabolites found in cellular extracts of yeast that share an excitation wavelength comparable to GFP and their presence leads to low signal-to-noise ratios. Much of the auto-fluorescence in yeast is due to flavins, a co enzymatic oxidation-reduction carrier, which absorb broadly in the violet–blue range (400–500 nm) and emit in the green (530 nm) ⁶⁷.

The yeast auto-fluorescence spectrum extends over hundreds of nanometers and contributes to loss of contrast and clarity in fluorescence detected techniques. Reducing auto-fluorescence (from both the sample and growth media) is necessary when using fluorescent proteins that have low fluorescent intensity. To reduce auto-fluorescence from the sample of interest, identification of the species likely responsible for auto-fluorescence can enable optimization of the experimental conditions to reduce its concentration or repress its ability to fluoresce.

Fortunately, multiple solutions are available to overcome the high amounts of auto-fluorescence found in yeast. By eliminating the background levels of fluorescent molecules, the GFP containing histone chaperones can be accurately

monitored and various sedimentation parameters will be determined by F-AUC. Unfortunately, auto-fluorescence cannot be completely eliminated. However, careful choice of yeast strain and growth conditions can reduce auto-fluorescence. Cells tend to be less fluorescent in early log phase ($OD_{600} \approx 0.2$). Rich yeast media are also highly auto-fluorescent and should be avoided. The major sources of auto-fluorescence are riboflavin and folic acid; omitting these components eliminates the media auto-fluorescence. Fortunately, most *S. cerevisiae* strains synthesize both auto-fluorescence vitamins. Therefore, removing these vitamins from the medium does not appear to introduce limitations. Cells should be grown in synthetic defined (S.D.) media to minimize auto-fluorescence. Affinity chromatography is used to purify and concentrate a substance from a mixture, and is an excellent solution to reducing high concentrations of intrinsically fluorescent molecules found in crude cell extracts. Alternatively, a counter stain, Evans Blue, works well. Evans Blue chemical dye, which fluoresces when excited with wavelengths between 470 and 540 nm, has an emission peak at 680 nm⁶⁸. The advantages are that the Evans Blue quenches the amount of naturally fluorescence molecules found in yeast by causing a shift in the auto-fluorescence wavelength.

We have collected preliminary data towards the end goal of characterizing endogenous histone chaperone complexes, as they exist in the cell. These studies have lead to the quantification of the fluorescent intensity and wavelength distribution of emission spectrum of our GFP-tagged histone chaperones. Additionally, this work proposes techniques to increase fluorescent signal to background ratios for future F-AUC investigations. Most importantly, these experiments demonstrate our capability to optimize fluorescence detection in order to use a very specialized instrument (one of the few in the world) to collect unique, innovative biochemical sedimentation data.

CHAPTER 7 FUTURE DIRECTIONS

7.1 SIGNIFICANCE

Histone chaperones and HATs are fundamental players in the regulation of chromatin dynamics and gene expression *in vivo*. Since the proteins in question are highly conserved in both sequence and function in all eukaryotes, understanding of the involvement of these complexes in the regulation of gene expression will provide significant findings that are directly linked to transcription. This is of particular interest since defects in histone acetyltransferases and chaperone function can easily result in the atypical regulation of gene transcription and ultimately the onset of human disease (including cancer). A greater understanding of the functional regulation of histone chaperones and HATs in gene transcription would be advantageous in selecting them for treatment of disease. Additionally, by determining that acetylation status of histones is vital for the regulation of transcription, allowing or preventing acetylation would be an effective therapeutic strategy. Furthermore, a complete understanding of histone chaperone-HAT interactions holds for a great potential for finding therapeutic intervention targets because errors in protein–protein interactions can manifest in human disease. By utilizing several powerful techniques, we are in a unique position to characterize the contribution of histone acetylation in transcriptional regulatory complexes and to profile the status of a specific modification in a unique way. We will examine the diversity of Nap1-HAT complexes, their functionality, and how they are regulated. Therefore, the identification of multi-protein complexes is a mechanism to better understand protein function and cell regulation. Thus, our study will provide new insights into the structure of chromatin and its regulation via posttranslational modifications of histone tails, which could be of interest to cancer, epigenetics, and drug design.

7.2 DISCUSSION

A complete understanding of the interplay between histone chaperones and HAT will reveal how they function together in the cell to regulate chromatin dynamics and ultimately gene expression. Our experiments used the well-characterized galactose inducible genes *GAL1*, *10* and *GAL7* of *S. cerevisiae* to study nucleosome occupancy before and after transcription initiation and histone eviction during gene transcription. We also reported acetylation status and acetylation kinetics at these genes before and after transcription initiation. By examining these properties in wild-type cells and then comparing them to deletion mutants of $\Delta nap1$, $\Delta vps75$, and $\Delta asf1$, we were able to elucidate possible roles for the histone chaperones in modifying chromatin structure.

Here we revealed the density of histone H3 in wild-type cells during repressive conditions is lower at promoter regions than coding regions. Interestingly, although we noticed different histone H3 eviction profiles at each amplicon, the overall patterns were comparable. We also observed higher rates of histone eviction at coding regions compared to the upstream regions. This behavior may be due to the higher initial density of nucleosomes at the coding regions.

Because histone acetylation has been implicated as a mark of active transcription, we queried the acetylation status at histone H3-K9 and H3-K14 at the promoter and coding regions of the *GAL* genes. In repressive conditions, we saw similar acetylation patterns at each amplicon. During transcription, we reported increased acetylation at all regions of each amplicon, with higher levels of acetylation occurring at promoter regions. Taken together, our data support the notions that nucleosome must be evicted for transcription to occur and that acetylation of histones is directly linked to gene activation.

We then observed the effects of deletion of the histone chaperone Nap1 at the *GAL1*, *10* and *GAL7* genes. We discovered a large decrease in H3 levels at both promoter and coding regions in the $\Delta nap1$ deletion strain. We also noticed a diminished ability for this strain to evict H3 as well as lowered eviction rates. Interestingly, we saw increased acetylation of histone H3K9 during repressive conditions, but decreased acetylation rates at this same residue. It is possible

that Nap1 is responsible for removing hyper-acetylated nucleosomes from the DNA during repressive conditions as well as recruiting the HAT responsible for acetylating histone H3-K9.

Next, we performed similar experiments in strains deleted for the histone chaperones $\Delta vps75$ and $\Delta asf1$. However, here we only profiled the promoter regions of our *GAL* genes. Similar to the $\Delta nap1$ strain, $\Delta vps75$ showed decreased histone H3 occupancy during repressive conditions as well as lowered eviction under activating conditions. We also reported hyper-acetylation of histone H3-K9 and H3-K14 in $\Delta vps75$ at inactive *GAL1*, 10 promoter regions coupled again with decreased acetylation rates during transcription. Interestingly, deletion of *ASF1* seemed to have little effect upon initial histone H3 occupancy or eviction. $\Delta asf1$ also had normal histone H3-K9 and H3-K14 acetylation levels at inactive promoter regions, but showed decreased acetylation rates at H3-K9 in activating conditions. These data suggest possible functional redundancy between Nap1 and Vps75, as both knockout mutants showed similar deviations from the behavior of the wild-type strain.

SUPPLEMENTAL TABLE 1: REAL TIME PCR OLIGOMERS USED FOR CHIP SAMPLE ANALYSIS

Amplicon Letter	Orientation	Real-Time PCR Amplicon	Real-Time PCR Sequence
A	Forward	GAL7 Coding	5'-CTA CCC ACC TTT ACT GAG AT-3'
	Reverse		5'-TAC AGT CTT TGT AGA TAA TG-3'
B	Forward	GAL7 UAS	5'-TCC TTT TGG AAA GCT ATA CT-3'
	Reverse		5'-ACT GTA TAG CCA GTC CTT CG-3'
C	Forward	GAL10 Coding	5'-CTA TTG GTA ACC ATA CAG TA-3'
	Reverse		5'-AAT AGT GTC TCC ATA TGG CT-3'
D	Forward	GAL10 Coding	5'-AGT TGC AGG TTG AAG ACT CC-3'
	Reverse		5'-ATC TGG TGC CGG CAC CAA TA-3'
E	Forward	GAL 10 5' ORF	5'-CAT AAG TTG AAT TCG ACA GG-3'
	Reverse		5'-GAC AGC TCA GTT ACA AAG TG-3'
F	Forward	GAL10 TATA Box	5'-CGG AAT TCG ACA GGT TAT CAG CA CA-3'
	Reverse		5'-GGG GCT CTT TAC ATT TCC ACA-3'
G	Forward	GAL1,10 UAS	5'-TGT TCG GAG CAG TGC TGC GC-3'
	Reverse		5'-ACG CTT AAC TGC TCA TTG CT-3'
H	Forward	GAL1 TATA Box	5'-CCA TAG GAT GAT AAT GCG AT-3'
	Reverse		5'-GG GCT CTT TAC ATT TCC ACA-3'
I	Forward	GAL1 5' ORF	5'-CCT CTA TAC TTT AAC GTC AAG G-3'
	Reverse		5'-CGG TTT AGC ATC ATA AGC GC-3'
J	Forward	GAL1 Coding	5'-CCA GTT GGT ACA TCA CCC TCA-3'
	Reverse		5'-ACT CTT CTG TGT CGG ACT GG-3'
K	Forward	GAL1 ORF	5'-CGT TCA TCA AGG CAC CAA AT-3'
	Reverse		5'-TCA GAG GGC TAA GCA TGT GT-3'
L	Forward	Telomere	5'-CGT AAC AAA GCC ATA ATG CC-3'
	Reverse		5'-CAG AAA GTA GTC CAG CCG-3'

SUPPLEMENTAL TABLE 2: WILD-TYPE HISTONE H3 OCCUPANCY AND EVICTION DATA
TABLE

Wild-Type Amplicon	Initial Histone H3 Occupancy (T_0)	Minimum Histone H3 Occupancy	Time of Minimum Occupancy	Time Independent Fold Eviction (Initial Occupancy/ Min. Occupancy)	Time Dependent Fold Eviction T_{20} (Initial Occupancy/ Histone Occupancy @ T_{20})	Time Dependent Fold Eviction T_{30} (Initial Occupancy/ Histone Occupancy @ T_{30})	Eviction Rate (Initial Histone Occupancy- Minimum Histone Occupancy)/ T_{min}	Tit
A Gal 7 Coding	10.01	2.33	60	8.88	4.85	4.21	3.06	
B Gal 7 UAS	11.78	0.50	60	23.56	4.82	11.08	1.88	
C Gal 10 Coding	19.35	2.42	60	8.00	3.47	4.06	2.82	
D Gal 10 Coding	18.46	4.27	30	4.37	1.75	2.07	4.73	
E Gal 10 5' ORF	10.81	2.82	60	3.83	1.77	2.63	1.33	
F Gal 10 TATA	20.70	2.38	60	8.70	3.77	6.27	3.05	
G Gal 1,10 UAS	10.81	1.62	60	6.67	2.77	4.00	1.53	
H Gal 1 TATA	13.13	2.13	60	6.16	2.72	3.25	1.83	
I Gal 1 5'ORF	14.89	2.41	60	6.18	2.68	2.84	2.08	
J Gal 1 Coding	16.23	3.15	60	5.12	2.06	2.42	2.18	

SUPPLEMENTAL TABLE 3: *Anap1* HISTONE H3 OCCUPANCY AND EVICTION TABLE

<i>Anap1</i> Amplicon	Initial Histone H3 Occupancy (T ₀)	Minimum Histone H3 Occupancy	Time of Minimum Occupancy	Time Independent Fold Eviction (Initial Occupancy/Min. Occupancy)	Time Dependent Fold Eviction T ₂₀ (Initial Occupancy/Histone Occupancy @ T ₂₀)	Time Dependent Fold Eviction T ₃₀ (Initial Occupancy/Histone Occupancy @ T ₃₀)	Eviction Rate (Initial Histone Occupancy-Minimum Histone Occupancy)/	Time To Reach Half Histone H3 Eviction (Minutes)
A Gal 7 Coding	11.82	3.94	30	3.00	2.55	3.00	2.62	16.5
B Gal 7 UAS	9.40	0.91	30	10.35	3.10	10.35	2.83	17.5
C Gal 10 Coding	7.23	3.27	30	2.21	1.70	2.21	1.32	18.5
D Gal 10 Coding	9.49	6.70	20	1.42	1.42	1.29	1.40	17.5
E Gal 10 5' ORF	8.87	3.98	60	2.23	1.15	2.16	0.82	23
F Gal 10 TATA	5.58	1.65	60	3.38	1.12	1.53	0.66	30
G Gal 1,10 UAS	7.74	1.53	30	5.04	2.29	5.04	2.07	17
H Gal 1 TATA	8.09	5.86	30	1.38	0.68	1.38	0.74	21
I Gal 1 5'ORF	7.57	2.36	30	3.20	1.41	3.20	1.74	20.5
J Gal 1 Coding	10.06	5.48	60	1.84	1.24	1.55	0.76	21.5
K Gal 1 Coding	9.63	5.52	30	1.74	1.46	1.74	1.37	18

SUPPLEMENTAL TABLE 4: *Avps75* HISTONE H3 OCCUPANCY AND EVICTION TABLE

<i>Avps75</i> Amplicon	Initial Histone H3 Occupancy (T_0)	Minimum Histone H3 Occupancy	Time of Minimum Occupancy (Minutes)	Time Dependent Fold Eviction T_{60} (Initial Occupancy/ Histone Occupancy @ T_{60})	Time Dependent Fold Eviction T_{30} (Initial Occupancy/ Histone Occupancy @ T_{30})	Eviction Rate (Initial Histone Occupancy- Minimum Histone Occupancy)/ T_{min}	Time To Reach Half Histone H3 Eviction (Minutes)
F Gal 10 TATA	8.85	5.8	60	1.53	0.78	0.51	53
G Gal 1,10 UAS	3.68	1.98	60	1.86	0.86	0.28	49

SUPPLEMENTAL TABLE 5: *Dasf1* HISTONE H3 OCCUPANCY AND EVICTION TABLE

<i>Dasf1</i> Amplicon	Initial Histone H3 Occupancy (T ₀)	Minimum Histone H3 Occupancy	Time of Minimum Occupancy (Minutes)	Time Dependent Fold Eviction T ₆₀ (Initial Occupancy/ Histone Occupancy @ T ₆₀)	Time Dependent Fold Eviction T ₃₀ (Initial Occupancy/ Histone Occupancy @ T ₃₀)	Eviction Rate (Initial Histone Occupancy- Minimum Histone Occupancy)/ T _{min}	Time To Reach Half Histone H3 Eviction (Minutes)
F Gal 10 TATA	19.6	4.64	30	2.67	4.23	4.99	15
G Gal 1,10 UAS	12.19	3.52	60	3.47	2.45	1.45	18

SUPPLEMENTAL TABLE 6: WILD-TYPE HISTONE H3 ACETYLATION (H3-K9/H3) TABLE

Amplicon Wild-Type	Initial Histone Acetylation (T ₀)	Max Histone Acetylation Observe	Time of Max Acetylation	Time Independent Fold Acetylation (Max Ac/ Initial Ac)	Time Dependent Fold Acetylation T20 (Ac @ T20/Initial Ac)	Time Dependent Fold Acetylation T30 (Ac @ T30/Initial Ac)	Acetylation Rate (Max Ac/T _{max})	T _{1/2} Acetylation Max (Minutes)	
A GAL 7 ORF	K9/H3	8.28	31.80	60	3.84	2.90	2.16	3.92	15
B GAL 7 UAS	K9/H3	13.54	87.67	20	6.47	6.28	5.97	37.07	14
C GAL 1,10 ORF II	K9/H3	11.51	61.32	20	5.33	5.33	2.62	24.9	8.5
D GAL 10 ORF I	K9/H3	10.27	23.11	10	2.25	2.03	1.88	12.84	4
E GAL 10 5' ORF	K9/H3	15.76	35.08	30	2.23	1.78	2.23	6.44	7
F GAL 10 TATA	K9/H3	12.59	69.40	60	5.51	2.69	3.49	9.47	27.5
G GAL 1,10 UAS	K9/H3	11.55	50.02	60	4.33	3.03	2.35	6.41	15.5
H GAL 1 TATA	K9/H3	11.99	47.75	60	3.98	3.14	2.00	5.96	11
I GAL 1 5' ORF	K9/H3	9.24	42.50	20	4.60	4.40	4.02	16.63	13
J GAL 1 ORF I	K9/H3	10.99	31.20	60	2.84	1.90	1.80	3.37	19.5
K GAL 1 ORF II	K9/H3	14.28	26.03	30	1.82	1.19	1.77	3.92	34.5

SUPPLEMENTAL TABLE 7: *Δnap1* HISTONE H3 ACETYLATION (H3-K9/H3) TABLE

Amplicon <i>Δnap1</i>	Acetylation Mark	Initial Histone Acetylation (T=0)	Max Histone Acetylation	Time of Max Acetylation	Time Independent Fold Acetylation (Max Ac/ Initial Ac)	Time Dependent Fold Acetylation T20 (Ac @ T20/ Initial Ac)	Time Dependent Fold Acetylation T30 (Ac @ T30/ Initial Ac)	Acetylation Rate (Max Ac-Initial Ac/ T _{max})	T _{1/2} Acetylation Max (Minutes)
A GAL 7 ORF	K9/H3	11.22	37.5	20	3.34	3.34	2.75	13.14	15
B GAL 7 UAS	K9/H3	22.2	142	30	6.40	2.81	6.40	39.93	22
C GAL 1,10 ORF II	K9/H3	26.1	65.7	30	2.52	1.72	2.52	13.2	20.5
D GAL 10 ORF I	K9/H3	21.9	36.5	30	1.67	1.34	1.67	4.87	20
E GAL 10 5' ORF	K9/H3	16.5	53.8	30	3.26	2.03	3.26	12.43	21
F GAL 10 TATA	K9/H3	22.5	68.3	30	3.04	2.04	3.03	15.27	20
G GAL 1,10 UAS	K9/H3	14.1	69	30	4.89	2.84	4.90	18.3	20.5
H GAL 1 TATA	K9/H3	15.2	45.7	60	3.01	1.37	2.71	5.08	24.5
I GAL 1 5' ORF	K9/H3	17.4	54.6	30	3.14	0.99	3.14	12.4	23.5

SUPPLEMENTAL TABLE 8: WILD-TYPE HISTONE H3 ACETYLATION (H3-K14/H3) TABLE

Amplicon Wild Type	Initial Histone Acetylation (T_0)	Max Histone Acetylation Observed	Time of Max Acetylation	Time Independent Fold Acetylation (Max Ac/Initial Ac)	Time Dependent Fold Acetylation T20 (Ac @ T20/Initial Ac)	Time Dependent Fold Acetylation T30 (Ac @ T30/Initial Ac)	Acetylation Rate (Max Ac-Initial Ac/ T_{max})	$T_{1/2}$ Acetylation Max (T_0 Dependent)	
A GAL 7 ORF	K14/H3	16.73	25.75	60	1.54	0.88	1.22	1.50	31
B GAL 7 UAS	K14/H3	16.82	67.70	30	4.02	2.70	3.96	16.96	18.5
C GAL 1,10 ORF II	K14/H3	15.79	48.07	20	3.04	2.82	2.55	16.14	13.5
D GAL 10 ORF I	K14/H3	18.92	40.18	30	2.12	1.69	2.12	7.08	10.5
E GAL 10 5' ORF	K14/H3	13.56	43.89	60	3.24	2.04	2.48	5.05	22
F GAL 10 TATA	K14/H3	14.85	64.30	60	4.33	1.63	3.52	8.24	23.5
G GAL 1,10 UAS	K14/H3	12.73	42.96	60	3.37	1.81	2.00	5.04	34
H GAL 1 TATA	K14/H3	11.67	37.49	60	3.21	2.22	2.24	4.30	16.5
I GAL 1 5' ORF	K14/H3	8.14	37.14	60	4.56	2.52	3.06	4.33	24.5
J GAL 1 ORF I	K14/H3	10.86	27.92	60	2.57	1.46	1.64	2.84	35.5
K GAL 1 ORF II	K14/H3	11.81	30.54	30	2.59	1.04	2.58	6.25	22.5

SUPPLEMENTAL TABLE 9: *Δnap1* HISTONE H3 ACETYLATION (H3-K14/H3) TABLE

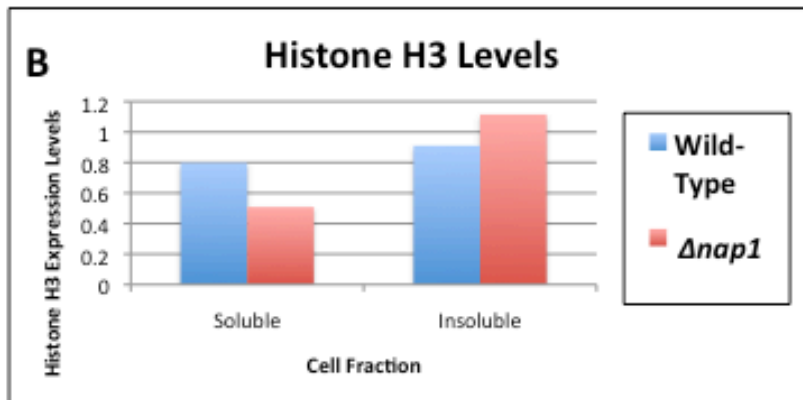
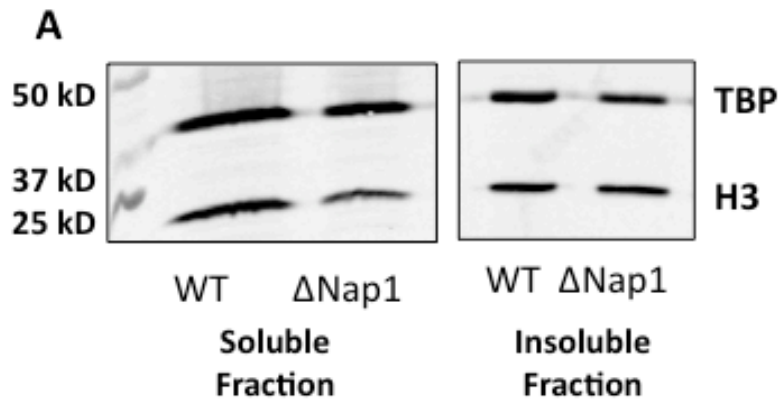
Amplicon <i>Δnap1</i>	Acetylation Mark	Initial Histone Acetylation (T ₀)	Max Histone Acetylation Observe	Time of Max Acetylation	Time Independent Fold Acetylation (Max Ac/ Initial Ac)	Time Dependent Fold Acetylation T20 (Ac @ T20/Initial Ac)	Time Dependent Fold Acetylation T30 (Ac @ T30/Initial Ac)	Acetylation Rate (Max Ac-Initial Ac/ T _{max})	T _{1/2} Acetylation Max (Minutes)
A GAL 7 ORF	K14/H3	14.1	34.4	20	2.44	2.44	2.08	10.15	8
B GAL 7 UAS	K14/H3	21.9	114.7	30	5.24	3.08	5.24	30.93	20
C GAL 1,10 ORF II	K14/H3	30.94	75.8	20	2.45	2.45	2.14	22.43	14.5
D GAL 10 ORF I	K14/H3	23.2	39.3	30	1.69	1.59	1.70	5.37	11.5
E GAL 10 5' ORF	K14/H3	14.5	39.6	30	2.73	1.8	2.66	8.37	9.5
F GAL 10 TATA	K14/H3	18.9	57.2	30	3.02	2.11	3.03	12.77	19
G GAL 1,10 UAS	K14/H3	12.17	56.2	30	4.62	3.12	4.62	14.68	18
H GAL 1 TATA	K14/H3	11.29	27.58	60	2.44	1.57	2.25	2.72	8
I GAL 1 5' ORF	K14/H3	12.2	41.9	30	3.43	3.29	3.43	9.9	14.5
J GAL 1 ORF I	K14/H3	9.11	31.03	20	3.41	3.40	2.46	10.96	10
K GAL I ORF II	K14/H3	12.48	22.9	30	1.83	1.94	1.83	3.47	14.5

SUPPLEMENTAL TABLE 10: $\Delta yps75$ HISTONE H3 ACETYLATION (H3-K9/H3 AND H3-K14/H3) TABLE

Amplicon <i>Δyps75</i>	Acetylation Mark	Initial Histone Acetylation (T ₀)	Max Histone Acetylation	Time of Max Acetylation	Time Dependent Fold Acetylation T30 (Ac @ T30/ Initial Ac)	Time Dependent Fold Acetylation T60 (Ac @ T60/ Initial Ac)	Acetylation Rate (Max Ac- Initial Ac/T _{max})
F GAL 10 TATA	K9/H3	23.45	31.51	30	1.34	1.15	2.68
F GAL 10 TATA	K14/H3	27.40	28.31	60	1.01	1.03	0.15
G GAL 1,10 UAS	K9/H3	28.90	35.38	30	1.22	0.67	2.16
G GAL 1,10 UAS	K14/H3	26.97	22.612	60	0.74	0.84	Ac Does Not In.

SUPPLEMENTAL TABLE 10: *Dasf1* HISTONE H3 ACETYLATION (H3-K9/H3 AND H3-K14/H3) TABLE

Amplicon <i>Dasf1</i>	Acetylation Mark	Initial Histone Acetylation (T ₀)	Max Histone Acetylation	Time of Max Acetylation	Time Dependent Fold Acetylation T20 (Ac @ T20/ Initial Ac)	Time Dependent Fold Acetylation T30 (Ac @ T30/ Initial Ac)	Acetylation Rate (Max Ac-Initial Ac/T _{max})
F GAL 10 TATA	K9/H3	16.50	76.49	60	1.65	4.63	10.00
F GAL 10 TATA	K14/H3	16.37	74.02	60	1.64	4.52	9.61
G GAL 1,10 UAS	K9/H3	8.96	23.97	60	1.66	2.68	2.50
G GAL 1,10 UAS	K14/H3	12.10	15.44	60	1.11	1.28	0.56



C

Strain	Soluble	Insoluble	Total
WT	0.798	0.910	1.708
Δ Nap1	0.507	1.115	1.621

SUPPLEMENTAL FIGURE 1: DELETION OF NAP1 HAS A MINIMAL AFFECT ON GLOBAL H3 EXPRESSION IN REPRESSIVE CONDITIONS
(A) 20 μ g of whole cell extracts from wild-type (WT) or strain deleted for *NAP1* (Δ nap1) were separated by 15% SDS gel electrophoreses, transferred to a nitrocellulose membrane, and probed with anti-H3 antibody. **(B-C)** Histone H3 expression levels were normalized to TBP levels and quantified.

REFERENCES

1. LUGER, K., MADER, A. W., RICHMOND, R. K., SARGENT, D. F. & RICHMOND, T. J. (1997). CRYSTAL STRUCTURE OF THE NUCLEOSOME CORE PARTICLE AT 2.8 Å RESOLUTION. *NATURE* 389, 251-60.
2. KORNBERG, R. D. & LORCH, Y. (1999). CHROMATIN-MODIFYING AND -REMODELING COMPLEXES. *CURR OPIN GENET DEV* 9, 148-51.
3. STERNER, D. E., GRANT, P. A., ROBERTS, S. M., DUGGAN, L. J., BELOTSEKOVSKAYA, R., PACELLA, L. A., WINSTON, F., WORKMAN, J. L. & BERGER, S. L. (1999). FUNCTIONAL ORGANIZATION OF THE YEAST SAGA COMPLEX: DISTINCT COMPONENTS INVOLVED IN STRUCTURAL INTEGRITY, NUCLEOSOME ACETYLATION, AND TATA-BINDING PROTEIN INTERACTION. *MOL CELL BIOL* 19, 86-98.
4. ANDREWS, A. J., CHEN, X., ZEVIN, A., STARGELL, L. A. & LUGER, K. THE HISTONE CHAPERONE NAP1 PROMOTES NUCLEOSOME ASSEMBLY BY ELIMINATING NONNUCLEOSOMAL HISTONE DNA INTERACTIONS. *MOL CELL* 37, 834-42.
5. PARK, Y. J. & LUGER, K. (2006). THE STRUCTURE OF NUCLEOSOME ASSEMBLY PROTEIN 1. *PROC NATL ACAD SCI USA* 103, 1248-53.
6. LUEBBEN, W. R., SHARMA, N. & NYBORG, J. K. NUCLEOSOME EVICTION AND ACTIVATED TRANSCRIPTION REQUIRE P300 ACETYLATION OF HISTONE H3 LYSINE 14. *PROC NATL ACAD SCI USA* 107, 19254-9.
7. KELLOGG, D. R., KIKUCHI, A., FUJII-NAKATA, T., TURCK, C. W. & MURRAY, A. W. (1995). MEMBERS OF THE NAP/SET FAMILY OF PROTEINS INTERACT SPECIFICALLY WITH B-TYPE CYCLINS. *J CELL BIOL* 130, 661-73.
8. PARK, Y. J., CHODAPARAMBIL, J. V., BAO, Y., MCBRYANT, S. J. & LUGER, K. (2005). NUCLEOSOME ASSEMBLY PROTEIN 1 EXCHANGES HISTONE H2A-H2B DIMERS AND ASSISTS NUCLEOSOME SLIDING. *J BIOL CHEM* 280, 1817-25.
9. ALTMAN, R. & KELLOGG, D. (1997). CONTROL OF MITOTIC EVENTS BY NAP1 AND THE GIN4 KINASE. *J CELL BIOL* 138, 119-30.
10. ASKREE, S. H., YEHUDA, T., SMOLIKOV, S., GUREVICH, R., HAWK, J., COKER, C., KRAUSKOPF, A., KUPIEC, M. & MCEACHERN, M. J. (2004). A GENOME-WIDE SCREEN FOR SACCHAROMYCES CEREVISIAE DELETION MUTANTS THAT AFFECT TELOMERE LENGTH. *PROC NATL ACAD SCI USA* 101, 8658-63.
11. BONANGELINO, C. J., CHAVEZ, E. M. & BONIFACINO, J. S. (2002). GENOMIC SCREEN FOR VACUOLAR PROTEIN SORTING GENES IN SACCHAROMYCES CEREVISIAE. *MOL BIOL CELL* 13, 2486-501.
12. SELTH, L. & SVEJSTRUP, J. Q. (2007). Vps75, A NEW YEAST MEMBER OF THE NAP HISTONE CHAPERONE FAMILY. *J BIOL CHEM* 282, 12358-62.
13. HAN, J., ZHOU, H., LI, Z., XU, R. M. & ZHANG, Z. (2007). THE RTT109-Vps75 HISTONE ACETYLTRANSFERASE COMPLEX ACETYLATED NON-NUCLEOSOMAL HISTONE H3. *J BIOL CHEM* 282, 14158-64.
14. SELTH, L. A., LORCH, Y., OCAMPO-HAFALLA, M. T., MITTER, R., SHALES, M., KROGAN, N. J., KORNBERG, R. D. & SVEJSTRUP, J. Q. (2009). AN RTT109-INDEPENDENT ROLE FOR Vps75 IN TRANSCRIPTION-ASSOCIATED NUCLEOSOME DYNAMICS. *MOL CELL BIOL*.

15. LE, S., DAVIS, C., KONOPKA, J. B. & STERNGLANZ, R. (1997). TWO NEW S-PHASE-SPECIFIC GENES FROM SACCHAROMYCES CEREVISIAE. *YEAST* 13, 1029-42.
16. ADKINS, M. W., HOWAR, S. R. & TYLER, J. K. (2004). CHROMATIN DISASSEMBLY MEDIATED BY THE HISTONE CHAPERONE ASF1 IS ESSENTIAL FOR TRANSCRIPTIONAL ACTIVATION OF THE YEAST *PHO5* AND *PHO8* GENES. *MOL CELL* 14, 657-66.
17. NAKATANI, Y., RAY-GALLET, D., QUIVY, J. P., TAGAMI, H. & ALMOUZZI, G. (2004). TWO DISTINCT NUCLEOSOME ASSEMBLY PATHWAYS: DEPENDENT OR INDEPENDENT OF DNA SYNTHESIS PROMOTED BY HISTONE H3.1 AND H3.3 COMPLEXES. *COLD SPRING HARB SYMP QUANT BIOL* 69, 273-80.
18. SCHWABISH, M. A. & STRUHL, K. (2006). ASF1 MEDIATES HISTONE EVICTION AND DEPOSITION DURING ELONGATION BY RNA POLYMERASE II. *MOL CELL* 22, 415-22.
19. KORBER, P., BARBARIC, S., LUCKENBACH, T., SCHMID, A., SCHERMER, U. J., BLASCHKE, D. & HORZ, W. (2006). THE HISTONE CHAPERONE ASF1 INCREASES THE RATE OF HISTONE EVICTION AT THE YEAST *PHO5* AND *PHO8* PROMOTERS. *J BIOL CHEM* 281, 5539-45.
20. JOHN, S., HOWE, L., TAFROV, S. T., GRANT, P. A., STERNGLANZ, R. & WORKMAN, J. L. (2000). THE SOMETHING ABOUT SILENCING PROTEIN, SAS3, IS THE CATALYTIC SUBUNIT OF NUA3, A γ TAF(II)30-CONTAINING HAT COMPLEX THAT INTERACTS WITH THE SPT16 SUBUNIT OF THE YEAST CP (Cdc68/Pob3)-FACT COMPLEX. *GENES DEV* 14, 1196-208.
21. SUKA, N., SUKA, Y., CARMEN, A. A., WU, J. & GRUNSTEIN, M. (2001). HIGHLY SPECIFIC ANTIBODIES DETERMINE HISTONE ACETYLATION SITE USAGE IN YEAST HETEROCHROMATIN AND EUCHROMATIN. *MOL CELL* 8, 473-9.
22. KUO, M. H., VOM BAUR, E., STRUHL, K. & ALLIS, C. D. (2000). GCN4 ACTIVATOR TARGETS GCN5 HISTONE ACETYLTRANSFERASE TO SPECIFIC PROMOTERS INDEPENDENTLY OF TRANSCRIPTION. *MOL CELL* 6, 1309-20.
23. ALLARD, S., UTLEY, R. T., SAVARD, J., CLARKE, A., GRANT, P., BRANDL, C. J., PILLUS, L., WORKMAN, J. L. & COTE, J. (1999). NUA4, AN ESSENTIAL TRANSCRIPTION ADAPTOR/HISTONE H4 ACETYLTRANSFERASE COMPLEX CONTAINING ESA1P AND THE ATM-RELATED COFACTOR TRA1P. *EMBO J* 18, 5108-19.
24. BABIARZ, J. E., HALLEY, J. E. & RINE, J. (2006). TELOMERIC HETEROCHROMATIN BOUNDARIES REQUIRE NUA4-DEPENDENT ACETYLATION OF HISTONE VARIANT H2A.Z IN *SACCHAROMYCES CEREVISIAE*. *GENES DEV* 20, 700-10.
25. FILLINGHAM, J., RECHT, J., SILVA, A. C., SUTER, B., EMILI, A., STAGLJAR, I., KROGAN, N. J., ALLIS, C. D., KEOGH, M. C. & GREENBLATT, J. F. (2008). CHAPERONE CONTROL OF THE ACTIVITY AND SPECIFICITY OF THE HISTONE H3 ACETYLTRANSFERASE RTT109. *MOL CELL BIOL* 28, 4342-53.
26. DRISCOLL, R., HUDSON, A. & JACKSON, S. P. (2007). YEAST RTT109 PROMOTES GENOME STABILITY BY ACETYLATED HISTONE H3 ON LYSINE 56. *SCIENCE* 315, 649-52.
27. GRANT, P. A., EBERHARTER, A., JOHN, S., COOK, R. G., TURNER, B. M. & WORKMAN, J. L. (1999). EXPANDED LYSINE ACETYLATION SPECIFICITY OF GCN5 IN NATIVE COMPLEXES. *J BIOL CHEM* 274, 5895-5900.
28. BALASUBRAMANIAN, R., PRAY-GRANT, M. G., SELLECK, W., GRANT, P. A. & TAN, S. (2002). ROLES OF THE ADA2 AND ADA3 TRANSCRIPTIONAL COACTIVATORS IN HISTONE ACETYLATION. *J BIOL CHEM.* 277, 7989-7995.
29. REINKE, H. & HORZ, W. (2003). HISTONES ARE FIRST HYPERACETYLATED AND THEN LOSE CONTACT WITH THE ACTIVATED *PHO5* PROMOTER. *MOL CELL* 11, 1599-607.

30. ZHAO, J., HERRERA-DIAZ, J. & GROSS, D. S. (2005). DOMAIN-WIDE DISPLACEMENT OF HISTONES BY ACTIVATED HEAT SHOCK FACTOR OCCURS INDEPENDENTLY OF SWI/SNF AND IS NOT CORRELATED WITH RNA POLYMERASE II DENSITY. *MOL CELL BIOL* 25, 8985-99.
31. JOHNSTON, M. (1987). A MODEL FUNGAL GENE REGULATORY MECHANISM: THE *GAL* GENES OF *SACCHAROMYCES CEREVISIAE*. *MICROBIOL. REV.* 51, 458-476.
32. JOHNSTON, M. & DAVIS, R. W. (1984). SEQUENCES THAT REGULATE THE DIVERGENT *GAL1-GAL10* PROMOTER IN *SACCHAROMYCES CEREVISIAE*. *MOL. CELL. BIOL.* 4, 1440-1448.
33. LOHR, D. & HOPPER, J. E. (1985). THE RELATIONSHIP OF REGULATORY PROTEINS AND DNASE I HYPERSENSITIVE SITES IN THE YEAST *GAL1-10* GENES. *NUCL. ACIDS RES.* 13, 8409-8423.
34. WEST, R. W., YOCUM, R. R. & PTASHNE, M. (1984). YEAST *GAL1-GAL10* DIVERGENT PROMOTER REGION: LOCATION AND FUNCTION OF THE UPSTREAM ACTIVATING SEQUENCE-UAS_G. *MOL. CELL. BIOL.* 4, 2467-2478.
35. ALLFREY, V. G., FAULKNER, R. & MIRSKY, A. E. (1964). ACETYLATION AND METHYLATION OF HISTONES AND THEIR POSSIBLE ROLE IN THE REGULATION OF RNA SYNTHESIS. *PROC NATL ACAD SCI USA* 51, 786-94.
36. HUH, W. K., FALVO, J. V., GERKE, L. C., CARROLL, A. S., HOWSON, R. W., WEISSMAN, J. S. & O'SHEA, E. K. (2003). GLOBAL ANALYSIS OF PROTEIN LOCALIZATION IN BUDDING YEAST. *NATURE* 425, 686-91.
37. STRAHL-BOLSINGER, S., HECHT, A., LUO, K. & GRUNSTEIN, M. (1997). SIR2 AND SIR4 INTERACTIONS DIFFER IN CORE AND EXTENDED TELOMERIC HETEROCHROMATIN IN YEAST. *GENES DEV* 11, 83-93.
38. ZHANG, L., FLETCHER, A., CHEUNG, V., WINSTON, F. & STARGELL, L. A. (2008). SPN1 REGULATES THE RECRUITMENT OF SPT6 AND THE SWI/SNF COMPLEX DURING TRANSCRIPTIONAL ACTIVATION BY RNA POLYMERASE II. *MOL CELL BIOL* 28, 1393-403.
39. CAVALLI, G. & THOMA, F. (1993). CHROMATIN TRANSITIONS DURING ACTIVATION AND REPRESSION OF GALACTOSE-REGULATED GENES IN YEAST. *EMBO J* 12, 4603-13.
40. WILLIAMS, S. K. & TYLER, J. K. (2007). TRANSCRIPTIONAL REGULATION BY CHROMATIN DISASSEMBLY AND REASSEMBLY. *CURR OPIN GENET DEV* 17, 88-93.
41. THIRIET, C. & HAYES, J. J. (2006). HISTONE DYNAMICS DURING TRANSCRIPTION: EXCHANGE OF H2A/H2B DIMERS AND H3/H4 TETRAMERS DURING POL II ELONGATION. *RESULTS PROBL CELL DIFFER* 41, 77-90.
42. GREGORY, P. D., SCHMID, A., ZAVARI, M., MUNSTERKOTTER, M. & HORZ, W. (1999). CHROMATIN REMODELLING AT THE PHO8 PROMOTER REQUIRES SWI-SNF AND SAGA AT A STEP SUBSEQUENT TO ACTIVATOR BINDING. *EMBO J* 18, 6407-14.
43. WORKMAN, J. & KINGSTON, R. (1998). ALTERATION OF NUCLEOSOME STRUCTURE AS A MECHANISM OF TRANSCRIPTIONAL REGULATION. *ANNU REV BIOCHEM* 67, 545-79.
44. LI, B., CAREY, M. & WORKMAN, J. L. (2007). THE ROLE OF CHROMATIN DURING TRANSCRIPTION. *CELL* 128, 707-19.
45. BIDDICK, R. K., LAW, G. L., CHIN, K. K. & YOUNG, E. T. (2008). THE TRANSCRIPTIONAL COACTIVATORS SAGA, SWI/SNF, AND MEDIATOR MAKE DISTINCT CONTRIBUTIONS TO ACTIVATION OF GLUCOSE-REPPRESSED GENES. *J BIOL CHEM* 283, 33101-9.
46. SCHWABISH, M. A. & STRUHL, K. (2007). THE SWI/SNF COMPLEX IS IMPORTANT FOR HISTONE EVICTION DURING TRANSCRIPTIONAL ACTIVATION AND RNA POLYMERASE II ELONGATION IN VIVO. *MOL CELL BIOL.*

47. ADKINS, M. W., WILLIAMS, S. K., LINGER, J. & TYLER, J. K. (2007). CHROMATIN DISASSEMBLY FROM THE *PHO5* PROMOTER IS ESSENTIAL FOR THE RECRUITMENT OF THE GENERAL TRANSCRIPTION MACHINERY AND COACTIVATORS. *MOL CELL BIOL* 27, 6372-82.
48. ADKINS, M. W. & TYLER, J. K. (2006). TRANSCRIPTIONAL ACTIVATORS ARE DISPENSABLE FOR TRANSCRIPTION IN THE ABSENCE OF SPT6-MEDIATED CHROMATIN REASSEMBLY OF PROMOTER REGIONS. *MOL CELL* 21, 405-16.
49. BOEGER, H., GRIESENBECK, J., STRATTAN, J. S. & KORNBERG, R. D. (2004). REMOVAL OF PROMOTER NUCLEOSOMES BY DISASSEMBLY RATHER THAN SLIDING IN VIVO. *MOL CELL* 14, 667-73.
50. DECKERT, J. & STRUHL, K. (2001). HISTONE ACETYLATION AT PROMOTERS IS DIFFERENTIALLY AFFECTED BY SPECIFIC ACTIVATORS AND REPRESSORS. *MOL CELL BIOL* 21, 2726-35.
51. BROWN, C. E., LECHNER, T., HOWE, L. & WORKMAN, J. L. (2000). THE MANY HATS OF TRANSCRIPTION COACTIVATORS. *TRENDS BIOCHEM SCI* 25, 15-9.
52. DE KONING, L., CORPET, A., HABER, J. E. & ALMOUZNI, G. (2007). HISTONE CHAPERONES: AN ESCORT NETWORK REGULATING HISTONE TRAFFIC. *NAT STRUCT MOL BIOL* 14, 997-1007.
53. AGEZ, M., CHEN, J., GUEROIS, R., VAN HEIJENOORT, C., THURET, J. Y., MANN, C. & OCHSENBEIN, F. (2007). STRUCTURE OF THE HISTONE CHAPERONE ASF1 BOUND TO THE HISTONE H3 C-TERMINAL HELIX AND FUNCTIONAL INSIGHTS. *STRUCTURE* 15, 191-9.
54. ANTczAK, A. J., Tsubota, T., KAUFMAN, P. D. & BERGER, J. M. (2006). STRUCTURE OF THE YEAST HISTONE H3-ASF1 INTERACTION: IMPLICATIONS FOR CHAPERONE MECHANISM, SPECIES-SPECIFIC INTERACTIONS, AND EPIGENETICS. *BMC STRUCT BIOL* 6, 26.
55. KIM, H. J., SEOL, J. H., HAN, J. W., YOUN, H. D. & CHO, E. J. (2007). HISTONE CHAPERONES REGULATE HISTONE EXCHANGE DURING TRANSCRIPTION. *EMBO J* 26, 4467-74.
56. RUFIANGE, A., JACQUES, P. E., BHAT, W., ROBERT, F. & NOURANI, A. (2007). GENOME-WIDE REPLICATION-INDEPENDENT HISTONE H3 EXCHANGE OCCURS PREDOMINANTLY AT PROMOTERS AND IMPLICATES H3 K56 ACETYLATION AND ASF1. *MOL CELL* 27, 393-405.
57. BERNDSEN, C. E., Tsubota, T., LINDNER, S. E., LEE, S., HOLTON, J. M., KAUFMAN, P. D., KECK, J. L. & DENU, J. M. (2008). MOLECULAR FUNCTIONS OF THE HISTONE ACETYLTRANSFERASE CHAPERONE COMPLEX RTT109-Vps75. *NAT STRUCT MOL BIOL* 15, 948-56.
58. JESSULAT, M., ALAMGIR, M., SALSALI, H., GREENBLATT, J., XU, J. & GOLSHANI, A. (2008). INTERACTING PROTEINS RTT109 AND VPS75 AFFECT THE EFFICIENCY OF NON-HOMOLOGOUS END-JOINING IN *SACCHAROMYCES CEREVISIAE*. *ARCH BIOCHEM BIOPHYS* 469, 157-64.
59. COLLINS, S. R., MILLER, K. M., MAAS, N. L., ROGUEV, A., FILLINGHAM, J., CHU, C. S., SCHULDINER, M., GEBBIA, M., RECHT, J., SHALES, M., DING, H., XU, H., HAN, J., INGVARSDOTTIR, K., CHENG, B., ANDREWS, B., BOONE, C., BERGER, S. L., HIETER, P., ZHANG, Z., BROWN, G. W., INGLES, C. J., EMILI, A., ALLIS, C. D., TOCZYSKI, D. P., WEISSMAN, J. S., GREENBLATT, J. F. & KROGAN, N. J. (2007). FUNCTIONAL DISSECTION OF PROTEIN COMPLEXES INVOLVED IN YEAST CHROMOSOME BIOLOGY USING A GENETIC INTERACTION MAP. *NATURE* 446, 806-10.

60. BROWN, P. H., BALBO, A. & SCHUCK, P. (2008). CHARACTERIZING PROTEIN-PROTEIN INTERACTIONS BY SEDIMENTATION VELOCITY ANALYTICAL ULTRACENTRIFUGATION. *CURR PROTOC IMMUNOL* CHAPTER 18, UNIT 18 15.
61. TSIEN, R. Y. (1998). THE GREEN FLUORESCENT PROTEIN. *ANNU REV BIOCHEM* 67, 509-44.
62. EDWARDS, A. N., FOWLKES, J. D., OWENS, E. T., STANDAERT, R. F., PELLETIER, D. A., HURST, G. B., DOKTYCZ, M. J. & MORRELL-FALVEY, J. L. (2009). AN IN VIVO IMAGING-BASED ASSAY FOR DETECTING PROTEIN INTERACTIONS OVER A WIDE RANGE OF BINDING AFFINITIES. *ANAL BIOCHEM* 395, 166-77.
63. TAICHMAN, R. S., WANG, Z., SHIOZAWA, Y., JUNG, Y., SONG, J., BALDUINO, A., WANG, J., PATEL, L. R., HAVENS, A. M., KUCIA, M., RATAJCZAK, M. Z. & KREBSBACH, P. H. PROSPECTIVE IDENTIFICATION AND SKELETAL LOCALIZATION OF CELLS CAPABLE OF MULTILINEAGE DIFFERENTIATION IN VIVO. *STEM CELLS DEV* 19, 1557-70.
64. LIU, N. A., REN, M., SONG, J., RIOS, Y., WAWROWSKY, K., BEN-SHLOMO, A., LIN, S. & MELMED, S. (2008). IN VIVO TIME-LAPSE IMAGING DELINEATES THE ZEBRAFISH PITUITARY PROOPIOMELANOCORTIN LINEAGE BOUNDARY REGULATED BY FGF3 SIGNAL. *DEV BIOL* 319, 192-200.
65. GHAEMMAGHAMI, S., HUH, W. K., BOWER, K., HOWSON, R. W., BELLE, A., DEPHOURE, N., O'SHEA, E. K. & WEISSMAN, J. S. (2003). GLOBAL ANALYSIS OF PROTEIN EXPRESSION IN YEAST. *NATURE* 425, 737-41.
66. SHEFF, M. A. & THORN, K. S. (2004). OPTIMIZED CASSETTES FOR FLUORESCENT PROTEIN TAGGING IN *SACCHAROMYCES CEREVISIAE*. *YEAST* 21, 661-70.
67. BENSON, R. C., MEYER, R. A., ZARUBA, M. E. & MCKHANN, G. M. (1979). CELLULAR AUTOFLUORESCENCE--IS IT DUE TO FLAVINS? *J HISTOCHEM CYTOCHEM* 27, 44-8.
68. HED, J., DAHLGREN, C. & RUNDQUIST, I. (1983). A SIMPLE FLUORESCENCE TECHNIQUE TO STAIN THE PLASMA MEMBRANE OF HUMAN NEUTROPHILS. *HISTOCHEMISTRY* 79, 105-10.